Computer Physics Communications 141 (2001) 175–204

Computer Physics Communications

www.elsevier.com/locate/cpc

Electronic structure calculation for N-electron quantum dots ☆

S.A. McCarthy, J.B. Wang *, P.C. Abbott

Department of Physics, The University of Western Australia, 35 Stirling Highway, Crawley, WA 6009, Australia

Accepted 17 June 2001

Abstract

The Hartree–Fock method for calculating the electronic structure of N-electron quantum dot systems was implemented in *Mathematica* using an easily understood modular code. Calculations were performed for quantum dot systems containing up to $N = 18$ electrons. The energy spectra obtained are in good agreement with those previously calculated using density functional theory. Qualitative agreement with an experimental spectrum is also obtained.

PACS: 73.20.Dx; 31.15.-p

Keywords: Hartree–Fock method; Quantum dot; Artificial atom; Electronic structure

PROGRAM SUMMARY

Title of program: QDHartreeFock.nb

Version number: 1.0

Catalogue identifier: ADPE

Program obtainable from: CPC Program Library, Queen's University of Belfast, N. Ireland

Program Summary URL: http://cpc.cs.qub.ac.uk/summaries/ADPE

Programming language used: Mathematica 4.1

Platform: Any platform supporting Mathematica 4.1 (tested using a remote kernel running on a DEC Alpha workstation 500 with 0.5 GB RAM)

Number of bytes in distributed program, including test data, etc.: 20 907

Distribution format: tar gzip file

Keywords: Hartree–Fock method, quantum dot, artificial atom, electronic structure

Nature of physical problem
Electronic structure of N-electrons confined in a quantum dot.

Method of solution
The Hartree–Fock self-consistent field method is applied to the physical problem. The Rayleigh–Ritz variational method is applied to solve the Hartree–Fock equations, using a mixture of analytic and numeric computational techniques.

Limitations
Restricted to circularly symmetric quantum dots; limited matrix (expansion) sizes.

Unusual features
A simple input structure. Analytic reduction of direct and exchange integrals speeds up computation and improves accuracy.

☆ This program can be downloaded from the CPC Program Library under catalogue identifier: http://cpc.cs.qub.ac.uk/summaries/ADPE

* Corresponding author.
E-mail address: wang@physics.uwa.edu.au (J.B. Wang).

0010-4655/01/$ – see front matter
PII: S0010-4655(01)00401-5

LONG WRITE-UP

1. Introduction

With the increased sophistication of semiconductor technology it is now possible to create man-made objects which display many of the characteristic properties normally associated with atoms. Electrons are trapped between two layers of semiconductor, effectively confining them to two-dimensions, and then restricted further by some lateral confining potential to create what has been termed an *artificial atom* or *quantum dot*. The ability of experimentalists to manipulate the size and shape of these artificial atoms has opened up a wide range of possibilities and areas for examination [1,2]. In the future, quantum dots may be used to build more efficient and precisely controlled lasers, and also as vital components of nanoelectronic devices [3,4]. It is also hoped that quantum dots may one day be able to help realize the dream of quantum computing [5].

Typical quantum dots of the type described in [1] can range in size from nanometers to a few microns and can contain anywhere from a few electrons to hundreds of electrons. The electrons are sandwiched between two layers of semiconductor, which typically have a spacing of approximately 0.5 nm. The lateral confining potential for a quantum dot with a large radius can be approximated as a finite square well with rounded edges. For a smaller dot however, we may instead model it as a smooth function, such as a Gaussian potential,

$$V(r) = -V_0 \mathrm{e}^{-r^2/R^2},$$

or a Pöschl–Teller potential,

$$V(r) = -V_0/\cosh^2\left(-r^2/R^2\right).$$

For states near the bottom of the well, a good approximation is that of a harmonic confining potential,

$$V(r) = -V_0 + \tfrac{1}{2}k^2 r^2.$$

The attraction of this harmonic model is that a simple analytic solution to the single electron Schrödinger equation exists [6,7].

The main focus of this paper is the calculation of the electronic states in quantum dots with N-electrons by applying the Hartree–Fock self-consistent field method. Pfannkuche et al. [8] performed Hartree–Fock calculations for a two-electron quantum dot (artificial helium), and compared with an exact solution to the two-electron system obtained by direct numerical diagonalization of the two-particle Hamiltonian. In this paper we extend the Hartree–Fock calculation to N-electron systems.

Ezaki et al. [9] applied a brute force approach by numerically diagonalizing the N-electron Hamiltonian using Slater determinants which were formed from the solutions to the single-electron problem. Lee et al. [10] also studied the N-electron problem, but applied a method based on density functional theory. Both groups obtained results in reasonable agreement with the experimental results reported by Tarucha et al. [11].

Most theoretical models in the literature, including Refs. [9,10], assume a harmonic confining potential when dealing with isotropic quantum dots. But what is the effect of altering this potential to something that is perhaps more realistic, such as the Gaussian or Pöschl–Teller potentials as suggested above? Section 2 starts by looking at this problem for a one electron quantum dot system, developing a general method which can be applied to a number of different potentials. We then describe the theory for the N-electron systems and present the associated Hartree–Fock equations to be solved. Section 3 presents the method of solution for the N-electron problem and a description of the developed code for the *Mathematica* package **QDHartreeFock.m**. Finally, Section 4 gives an example and some results obtained using this program.

2. Theory

2.1. Single electron systems

In our model of quantum dot systems, we assume that the confining potential can be separated into a vertical (z) component and a lateral ($\boldsymbol{r} = (r, \phi)$) component. The confining potential in the vertical direction can be thought of as effectively being a very narrow infinite triangular well [12], whereas the lateral confining potential $V(\boldsymbol{r})$ has a bowl-like shape. The energy level of the first excited state in the z direction is generally hundreds of times greater than many of the low energy states in the r-ϕ plane. This property allows us to model electron motion in a quantum dot as two-dimensional. Thus the Schrödinger equation in plane polar coordinates reads

$$\left(-\frac{\hbar^2}{2m^*}\nabla_{\boldsymbol{r}}^2 + V(\boldsymbol{r})\right)\psi(\boldsymbol{r}) = \mathcal{E}\psi(\boldsymbol{r}),$$

where m^* is the effective mass, and ∇_r^2 is the two-dimensional Laplacian. We now switch to rescaled atomic units by setting $\hbar = m^* = e = a_0^* = 1$, with $a_0^* = 4\pi\epsilon\hbar^2/m^*e^2$ the effective Bohr radius, and ϵ the dielectric constant. Assuming a circularly symmetric confining potential $V(r, \phi) \equiv V(r)$, and using separation of variables, we see that $\psi(r, \phi) = \frac{1}{\sqrt{2\pi}}\mathrm{e}^{\mathrm{i}m\phi}R(r)$ with $R(r)$ satisfying the radial equation,

$$\left(-\frac{1}{2r}\frac{\partial}{\partial r}\left(r\frac{\partial}{\partial r}\right) + \frac{m^2}{2r^2} + V(r)\right)R(r) = \mathcal{E}R(r), \tag{1}$$

where $m \in \mathbb{Z}$ is a quantum number related to the orbital angular momentum of the system [13].

For the case of a harmonic confining potential of the form $V(r) = -V_0 + \frac{1}{2}k^2r^2$, there exists a simple analytic solution to Eq. (1) [6,7]. The solution is

$$R_{n,|m|}(r) = A_{n,|m|}r^{|m|}\mathrm{e}^{-kr^2/2}L_n^{|m|}(kr^2), \quad m \in \mathbb{Z},\ n = 0, 1, 2, \ldots, \tag{2}$$

where $A_{n,|m|}$ are normalization constants, and $L_n^{|m|}(x)$ are the generalized Laguerre polynomials [14]. The corresponding energy eigenvalues are given by

$$\mathcal{E}_{n,|m|} = k\big(2n + |m| + 1\big) - V_0. \tag{3}$$

Notice that we now have two quantum numbers, corresponding to the fact that we are dealing with a two-dimensional system. The spin quantum number is $\pm 1/2$. With no magnetic field, each of the above energy eigenstates is actually two-fold degenerate.

2.2. Rayleigh–Ritz variational technique

We would like to be able to solve Eq. (1) for a number of different confining potentials $V(r)$. To accomplish this we use the Rayleigh–Ritz variational technique. The Rayleigh–Ritz variational principle can be used to solve differential eigenvalue equations by expanding the unknown function in terms of a set of basis functions, and then reducing the problem to a matrix eigenvalue problem. For completeness we present the basic theory here. We begin with an equation of the form

$$\mathcal{L}u_n(\boldsymbol{x}) = \lambda_n u_n(\boldsymbol{x}),$$

where $x \in \mathbb{R}^n$, $\mathcal{L}$ is some linear differential operator, $u_n(\boldsymbol{x})$ are the eigenfunctions, and λ_n are the eigenvalues. The problem can also be formulated as a functional equation,

$$\lambda[\phi] = \frac{\int \phi^*(\boldsymbol{x})\mathcal{L}\phi(\boldsymbol{x})\,\mathrm{d}\boldsymbol{x}}{\int \phi^*(\boldsymbol{x})\phi(\boldsymbol{x})\,\mathrm{d}\boldsymbol{x}}. \tag{4}$$

It is easy to see that if ϕ is an eigenfunction of $\mathcal{L}$, say $\phi = u_n$, then $\lambda[\phi]$ will be the eigenvalue λ_n. It can also be shown that if some function ϕ causes $\lambda[\phi]$ to become stationary, i.e.

$$\frac{\delta\lambda[\phi]}{\delta\phi} = 0,$$

then ϕ is an eigenfunction of $\mathcal{L}$ [15]. Alternatively, expanding ϕ in terms of a complete set of basis functions $v_i(x)$, so that

$$\phi(\boldsymbol{x}) = \sum_{i=1}^{\infty} c_i v_i(\boldsymbol{x}) \equiv \boldsymbol{c}^{\mathrm{T}}\boldsymbol{v}(\boldsymbol{x}),$$

where $\{\boldsymbol{c}\}_i = c_i$, and $\{\boldsymbol{v}(\boldsymbol{x})\}_i = v_i(\boldsymbol{x})$, Eq. (4) becomes

$$\lambda[\phi] = \frac{\sum_{i,j} c_i^* c_j \int v_i^*(\boldsymbol{x})\mathcal{L}v_j(\boldsymbol{x})\,\mathrm{d}\boldsymbol{x}}{\sum_{i,j} c_i^* c_j \int v_i^*(\boldsymbol{x})v_j(\boldsymbol{x})\,\mathrm{d}\boldsymbol{x}}. \tag{5}$$

Introducing the *Ritz matrix* $\mathcal{A}$,

$$\{\mathcal{A}\}_{ij} = \int v_i^*(\boldsymbol{x})\mathcal{L}v_j(\boldsymbol{x})\,\mathrm{d}\boldsymbol{x}, \tag{6}$$

and the *overlap matrix* $\mathcal{B}$,

$$\{\mathcal{B}\}_{ij} = \int v_i^*(\boldsymbol{x})v_j(\boldsymbol{x})\,\mathrm{d}\boldsymbol{x}, \tag{7}$$

Eq. (5) reads

$$\lambda[\phi] = \frac{\boldsymbol{c}^{\dagger}\mathcal{A}\boldsymbol{c}}{\boldsymbol{c}^{\dagger}\mathcal{B}\boldsymbol{c}}.$$

Variation of Eq. (5) with respect to the expansion coefficients

$$\frac{\delta\lambda[\phi]}{\delta c_i} = 0,$$

leads to the generalized matrix eigenvalue equation, known as the Ritz (matrix) equation

$$\mathcal{A}\boldsymbol{c} = \lambda\mathcal{B}\boldsymbol{c}.$$

In general $\mathcal{A}$ and $\mathcal{B}$ are infinite dimensional matrices. Truncating $\mathcal{A}$ and $\mathcal{B}$ to $\mathcal{N}\times\mathcal{N}$ matrices, the resulting $\mathcal{N}$-dimensional matrix eigenvalue problem,

$$\left(\mathcal{B}_{\mathcal{N}}^{-1}\mathcal{A}_{\mathcal{N}}\right)\boldsymbol{c}_{\mathcal{N}} = \lambda\boldsymbol{c}_{\mathcal{N}}, \tag{8}$$

can be solved for non-singular $\mathcal{B}_{\mathcal{N}}$. As a result of this truncation, the eigenvectors and eigenvalues are now approximations to the actual solutions,

$$\phi(\boldsymbol{x}) \simeq \phi_{\mathcal{N}}(\boldsymbol{x}) = \sum_{i=1}^{\mathcal{N}} c_i v_i(\boldsymbol{x}) \equiv \boldsymbol{c}_{\mathcal{N}}^{\mathrm{T}}\boldsymbol{v}_{\mathcal{N}}(\boldsymbol{x}).$$

As we increase $\mathcal{N}$, we converge to the exact eigenvectors and eigenvalues, with the condition that

$$\lambda_{\mathrm{exact}} \leqslant \lambda[\phi_{\mathcal{N}}],$$

implying that $\lambda[\phi_{\mathcal{N}}]$ is an upper bound for the exact eigenvalues of $\mathcal{L}$ [15].

2.3. Example: Gaussian confining potential

As an example of a non-harmonic confining potential, consider the Gaussian potential of the form $V(r) = -V_0 e^{-r^2/R^2}$. The attraction of this potential is the smooth nature of the Gaussian function near the top of the well. This avoids any edge effects which may affect other model potentials.

Unlike the harmonic case, simple analytic solutions to this equation are not known. To solve by applying the Rayleigh–Ritz variational method, we first find a suitable set of basis functions to expand $R(r)$. For small r, the confining potential $V(r)$ behaves like r^2,

$$V(r) = -V_0 e^{-r^2/R^2} = -V_0 + \frac{V_0 r^2}{R^2} + O(r^4).$$

Consequently, if we expand $R(r)$ in terms of the solutions to the harmonic oscillator problem given by Eq. (2), we can expect rapid convergence for at least the lowest energies which occupy the bottom of the well. We link the values of V_0 and R to the value of k in the harmonic oscillator potential by identifying $k = \sqrt{2V_0/R^2}$ in the set of basis functions,

$$v_{i,m}(r) = r^m e^{-kr^2/2} L_i^m(kr^2),$$

where, for convenience, we let $m = |m| \in \mathbb{N}$. The ijth matrix element of the $\mathcal{N} \times \mathcal{N}$ Ritz matrix given by Eq. (6) is

$$\{\mathcal{A}\}_{ij} = 2\pi \int_0^\infty \left(\frac{1}{2} v_{i,m}^{*\prime}(r) v_{j,m}^{\prime}(r) + \left(\frac{m^2}{2r^2} - V_0 e^{-r^2/R^2} \right) v_i^*(r) v_j(r) \right) r \, dr, \tag{9}$$

and the ijth matrix element of the $\mathcal{N} \times \mathcal{N}$ overlap matrix given by Eq. (7) is

$$\{\mathcal{B}\}_{i,j} = 2\pi \int_0^\infty v_{i,m}^*(r) v_{j,m}(r) r \, dr. \tag{10}$$

Note that the volume element is $d\boldsymbol{x} = r \, dr \, d\phi$, since we are working in two dimensions. The 2π factor results from the integration over ϕ. The details of the analytic evaluation of the integrals in Eqs. (9) and (10) is presented in Appendices B and C.

With these integrals, we can now solve the generalized matrix eigenvalue problem, Eq. (8). In fact we essentially have an analytic solution to the problem of the Gaussian well in that we know the value of each of the matrix elements of $\mathcal{A}$ and $\mathcal{B}$, and can thus determine the solutions to arbitrary accuracy by truncating the matrices to some suitable $\mathcal{N}$.

The energy levels of the Gaussian potential and, for comparison, the harmonic potential are plotted in Fig. 1. We observe that the general effect of the Gaussian potential compared to the harmonic potential is a lowering of corresponding energy states—this effect becoming more pronounced towards the top of the well, as expected. We also notice that we lose some of the degeneracy associated with the harmonic potential. For example, the states $\{n, m\} = \{1, 0\}$ and $\{0, \pm 2\}$ are degenerate in the harmonic potential, but split in the Gaussian potential. As we increase the matrix size, we get a higher density of states towards the top of the potential, as expected for the required transition to the continuum that exists for positive energy. These results agree with those presented by Adamowski et al. [16].

The method developed here is applicable to many different forms of potential. Even if an analytic solution for the integral involving $V(r)$ is not obtainable, numerical integration is usually practicable.

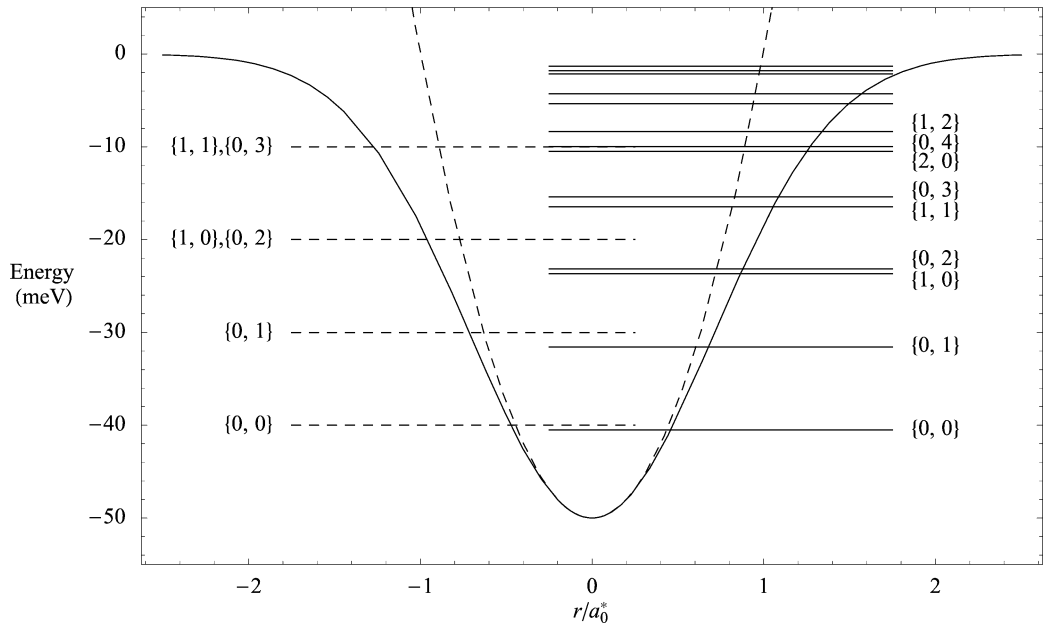

Fig. 1. Energy levels for a single electron in the Gaussian $V(r) = -V_0 e^{-r^2/R^2}$ (solid lines) and harmonic $V(r) = -V_0 + \frac{1}{2}k^2r^2$ (dashed lines) confining potentials, for $V_0 = 50$ and $k = 10$, while $R = \sqrt{2V_0/k^2}$. The states are labeled by $\{n, m\}$ and the two potentials are also plotted as functions of r. Calculations were performed with a matrix size of $\mathcal{N} = 20$.

2.4. *N*-electron systems

We now turn to the problem of an N-electron quantum dot system. The N-electron non-relativistic Hamiltonian in plane polar coordinates $\boldsymbol{r} = (r, \phi)$ is

$$\mathcal{H} = \mathcal{H}_1 + \mathcal{H}_2 = \sum_{i=1}^{N}\left(-\frac{\hbar^2}{2m^*}\nabla_{\boldsymbol{r}_i}^2 + V(\boldsymbol{r}_i)\right) + \sum_{i>j=1}^{N}\frac{e^2}{4\pi\epsilon}\frac{1}{r_{ij}},$$

where $r_{ij} = |\boldsymbol{r}_i - \boldsymbol{r}_j|$, m^* is the effective mass of the electron, and ϵ is the dielectric constant (for GaAs $m^* \simeq 0.065m_e$ and $\epsilon \simeq 12.9\epsilon_0$). We have separated the Hamiltonian into two parts: $\mathcal{H}_1$, which is a one-electron operator representing the kinetic energy terms and $\mathcal{H}_2$, which is a two-electron operator representing the interaction potential.

In rescaled atomic units the Schrödinger equation for the N-electron system is then

$$\left[\sum_{i=1}^{N}\left(-\frac{1}{2}\nabla_{r_i}^2 + V(\boldsymbol{r}_i)\right) + \sum_{i>j=1}^{N}\frac{1}{r_{ij}}\right]\Psi(q_1, q_2, \ldots, q_N) = \mathcal{E}\Psi(q_1, q_2, \ldots, q_N),$$

where q_i represents collectively both the spatial coordinate $\boldsymbol{r}_i$ and the spin coordinate of the ith electron.

2.5. Hartree–Fock equations

To solve the N-electron Schrödinger equation we use the Hartree–Fock method [15]. The Hartree–Fock approach is a particular case of the variational method, in which the trial wavefunction is assumed to be a $N \times N$ Slater determinant,

$$\Psi(q_1, q_2, \ldots, q_N) = \frac{1}{\sqrt{N!}} \begin{vmatrix} \psi_\alpha(q_1) & \psi_\beta(q_1) & \cdots & \psi_\nu(q_1) \\ \psi_\alpha(q_2) & \psi_\beta(q_2) & \cdots & \psi_\nu(q_2) \\ \vdots & \vdots & \ddots & \vdots \\ \psi_\alpha(q_N) & \psi_\beta(q_N) & \cdots & \psi_\nu(q_N) \end{vmatrix},$$

where the symbols $\alpha, \beta, \ldots, \nu$ correspond to the N-particle states labeled by the three quantum numbers $\{n, m, m_S\}$, and $\psi_\lambda(q_i)$ are the individual electron spin-orbitals.

Using these definitions, the Hartree–Fock equation for the ith electron in the state λ is

$$\left(-\frac{1}{2}\nabla_{\boldsymbol{r}_i}^2 + V(\boldsymbol{r}_i) + \mathcal{V}_\lambda^d(\boldsymbol{r}_i) - \mathcal{V}_\lambda^{\mathrm{ex}}(q_i)\right)\psi_\lambda(q_i) = \mathcal{E}_\lambda \psi_\lambda(q_i), \tag{11}$$

where the Coulomb direct potential $\mathcal{V}_\lambda^d(\boldsymbol{r}_i)$ represents the *average potential* due to the $N-1$ other electrons, and the exchange potential $\mathcal{V}_\lambda^{\mathrm{ex}}(q_i)$ represents an *exchange term* due to spin interactions. These two potentials are given by

$$\mathcal{V}_\lambda^d(\boldsymbol{r}_i) = \sum_{\mu\neq\lambda} \mathcal{V}_\mu^d(\boldsymbol{r}_i) = \sum_{\mu\neq\lambda} \int \frac{|\psi_\mu(\boldsymbol{r}_j)|^2}{r_{ij}}\,\mathrm{d}\boldsymbol{r}_j, \tag{12}$$

and

$$\mathcal{V}_\lambda^{\mathrm{ex}}(q_i)\psi_\lambda(q_i) = \sum_{\mu\neq\lambda} \delta_{m_S^\mu, m_S^\lambda} \left(\int \frac{\psi_\mu^*(\boldsymbol{r}_j)\psi_\lambda(\boldsymbol{r}_j)}{r_{ij}}\,\mathrm{d}\boldsymbol{r}_j\right)\psi_\mu(\boldsymbol{r}_i)\chi_{1/2,m_S^\mu}, \tag{13}$$

where $\chi_{1/2,m_S^\mu}$ is a spin function. (Note that $\sum_{\mu\neq\lambda}$ is a sum over all the N occupied states $\mu = \alpha, \beta, \ldots, \nu$, such that $\mu \neq \lambda$, where λ is the state occupied by the ith electron.) $\mathcal{E}_\lambda$ can be interpreted as energy required to remove an electron form the spin orbital ψ_λ, or the *ionization energy* of the electron in the state λ (Koopman's Theorem).

3. Solution and implementation with *Mathematica*

We now develop a method for solving the Hartree–Fock equations self-consistently with *Mathematica*.

Note. In the below definitions, $\mathcal{S}$ is the list defining the state of each of the N electrons, λ is the state $\{n, m, m_S\}$ of the electron being solved for, $\mathcal{N}$ is the number of terms in the expansion, and η is the current iteration loop.

3.1. Initialization

We first turn off some warning messages, and define a few useful notations for the direct and exchange integrals.

```
In[1] := Off[General :: "spell"]; Off[General :: "spell1"];
In[2] := Needs["Utilities`Notation`"]
In[3] := SetOptions[Notation, WorkingForm → TraditionalForm];
In[4] := Notation[ℐ^d_{i_,j_}[λ_, 𝒮_, 𝒩_, k_, η_] ⟺ CoulombIntegral[i_, j_, λ_, 𝒮_, 𝒩_, k_, η_]]
In[5] := Notation[ℐ^ex_{i_,j_}[λ_, 𝒮_, 𝒩_, k_, η_] ⟺ ExchangeIntegral[i_, j_, λ_, 𝒮_, 𝒩_, k_, η_]]
```

3.2. Simplification of the Hartree–Fock equations

We start by considering the direct and exchange potentials, Eqs. (12) and (13). These simplify if we make the assumption that the wavefunction for the ith electron in the state λ is of the form

$$\psi_\lambda(r_i,\phi_i) = R_\lambda(r_i)\frac{\mathrm{e}^{\mathrm{i}m^\lambda\phi_i}}{\sqrt{2\pi}}. \tag{14}$$

This assumption is valid for systems with complete subshells, and is a good approximation for incomplete subshells [15]. Expanding r_{ij} into its explicit dependence on r_i, r_j, and $\phi = \phi_{ij} = \phi_j - \phi_i$ (angle between $\boldsymbol{r}_i$ and $\boldsymbol{r}_j$) we obtain

$$r_{ij} = |\boldsymbol{r}_i - \boldsymbol{r}_j| = \left(r_i^2 + r_j^2 - 2r_i r_j\cos(\phi)\right)^{1/2} = r_>\left(1+\rho^2 - 2\rho\cos(\phi_j-\phi_i)\right)^{1/2}, \tag{15}$$

where $r_> = \max\{r_i,r_j\}$, $r_< = \min\{r_i,r_j\}$, $\rho = r_</r_>$ and $0 \leqslant \rho < 1$. Then we can perform the integration over ϕ (see Appendix A for details), which gives us simplified forms for the $\mathcal{V}_\lambda^d$ and $\mathcal{V}_\lambda^{\mathrm{ex}}$ terms. Eq. (11) now becomes the radial Hartree–Fock equation which reads

$$\left(-\frac{1}{2r_i}\frac{\partial}{\partial r_i}\left(r_i\frac{\partial}{\partial r_i}\right) + \frac{(m^\lambda)^2}{2r_i^2} + V(r_i) + \mathcal{V}_\lambda^d(r_i) - \mathcal{V}_\lambda^{\mathrm{ex}}(r_i)\right)R_\lambda(r_i) = \mathcal{E}_\lambda R_\lambda(r_i), \tag{16}$$

with

$$\mathcal{V}_\lambda^d(r) = \frac{1}{2\pi}\sum_{\mu\neq\lambda}\int_0^\infty |R_\mu(r\xi)|\frac{\mathfrak{V}_0(\xi)}{|1-\xi|}r\xi\,\mathrm{d}\xi, \tag{17}$$

$$\mathcal{V}_\lambda^{\mathrm{ex}}(r)R_\lambda(r) = \frac{1}{2\pi}\sum_{\mu\neq\lambda}\delta_{m_S^\mu,m_S^\lambda}R_\mu(r)\int_0^\infty R_\mu^*(r\xi)R_\lambda(r\xi)\frac{\mathcal{V}_m(\xi)}{|1-\xi|}r\xi\,\mathrm{d}\xi, \tag{18}$$

where $m = m^\lambda - m^\mu \in \mathbb{Z}$ with $\xi = r_j/r_i$. The factor $1/|1-\xi|$ results from the integration over ϕ and highlights the singularity at $\xi = 1$ (i.e. $r_i = r_j$). The terms $\mathfrak{V}_m(\xi)$ are polynomials involving elliptic integrals. The first three functions are

$$\mathfrak{V}_0(\xi) = 4K\left(-\frac{4\xi}{(\xi-1)^2}\right),$$

$$\mathfrak{V}_1(\xi) = \frac{2\left((\xi^2+1)K\left(-\frac{4\xi}{(\xi-1)^2}\right) - (\xi-1)^2E\left(-\frac{4\xi}{(\xi-1)^2}\right)\right)}{\xi},$$

and

$$\mathfrak{V}_2(\xi) = \frac{4\left((\xi^4+\xi^2+1)K\left(-\frac{4\xi}{(\xi-1)^2}\right) - (\xi-1)^2(\xi^2+1)E\left(-\frac{4\xi}{(\xi-1)^2}\right)\right)}{3\xi^2},$$

where $K(x)$ and $E(x)$ are the complete elliptic integrals of the first and second kinds, respectively [17]. Computer packages, such as *Mathematica*, are able to obtain these functions relatively easily.

In[6] :=

$$\mathfrak{V}\,/.\,\mathfrak{V}_{m\_} := \mathfrak{V}\,/.\,\mathfrak{V}_m$$

$$= \mathbf{Function}\Big[\{\xi\}, \mathbf{Evaluate}\Big[\mathbf{FullSimplify}\Big[\mathbf{Collect}\Big[\mathbf{Simplify}\Big[(1-\xi)\int_0^{2\pi}\frac{\cos(m\phi)}{\sqrt{\xi^2-2\cos(\phi)\xi+1}}\,\mathrm{d}\phi,\ 0\leqslant\xi<1\Big],$$

$$\{K(\_), E(\_), \xi\}, \mathbf{Simplify}\Big]\Big]\Big]\Big]$$

In[7] := **Table[$\mathfrak{V}_m(\xi)$, {m, 0, 2}] // TableForm**

Out[7] // TableForm =

$$4K\left(-\frac{4\xi}{(\xi-1)^2}\right)$$

$$\frac{2\left((\xi^2+1)K\left(-\frac{4\xi}{(\xi-1)^2}\right)-(\xi-1)^2E\left(-\frac{4\xi}{(\xi-1)^2}\right)\right)}{\xi}$$

$$\frac{4\left((\xi^4+\xi^2+1)K\left(-\frac{4\xi}{(\xi-1)^2}\right)-(\xi-1)^2(\xi^2+1)E\left(-\frac{4\xi}{(\xi-1)^2}\right)\right)}{3\xi^2}$$

Note the *dynamic programming* syntax, $\mathfrak{V}$ /: $\mathfrak{V}_{m\_} := \mathfrak{V}$ /: $\mathfrak{V}_m = \cdots$, which stores the values of $\mathfrak{V}_m$ under the symbol $\mathfrak{V}$ as they are evaluated.

3.3. Application of the Rayleigh–Ritz variational technique

To solve Eq. (16), we apply the Rayleigh–Ritz variational method as described in §2.2, by expanding $R_\lambda(r_i)$ in terms of a complete set of basis functions $v_{i,m^\lambda}(r)$, and then truncating the expansion after $\mathcal{N}$ terms,

$$R_\lambda(r) = \sum_{i=0}^{\mathcal{N}_1} c_{i,m^\lambda} v_{i,m^\lambda}(r), \tag{19}$$

with $c_{i,m}$ suitably chosen to normalize R. As our choice of basis functions we use the solutions of a single electron in a two-dimensional harmonic confining potential given by Eq. (2),

$$v_{i,m}(r) = r^m \mathrm{e}^{-kr^2/2} L_i^m(kr^2), \tag{20}$$

which we implement in *Mathematica* as

In[8] := **v /: $v_{i\_,m\_}$ = Function[{k, r}, $\mathrm{e}^{-\frac{k}{2}r^2} r^m L_i^m(kr^2)$];**

Following §2.2, the ijth matrix element of the $\mathcal{N}\times\mathcal{N}$ Ritz matrix given by Eq. (6) is

$$\{\mathcal{A}\}_{ij} = \alpha_{ij} + \mathcal{V}_{ij} + \mathcal{I}^d_{ij} - \mathcal{I}^{\mathrm{ex}}_{ij},$$

where α_{ij} are the kinetic energy integrals, $\mathcal{V}_{ij}$ are the confining potential integrals, and $\mathcal{I}^d_{ij}$, $\mathcal{I}^{\mathrm{ex}}_{ij}$ are the direct and exchange integrals. The ijth matrix element of the $\mathcal{N}\times\mathcal{N}$ overlap matrix given by Eq. (7) is

$$\{\mathcal{B}\}_{ij} = \beta_{ij},$$

where β_{ij} are the overlap integrals.

In *Mathematica* we form the $\mathcal{A}$ and $\mathcal{B}$ matrices of dimension $\mathcal{N}$ by

In[9] := **$\mathcal{A}$ /: $\mathcal{A}_{\mathcal{N}\_}$:= Function[{λ, $\mathcal{S}$, k, V0, η},**
Table[$\alpha_{i,j}$[k, |λ[[2]]|] + $\mathcal{V}_{i,j}$[k, V0, |λ[[2]]|] + $\mathcal{I}^d_{i,j}$[λ, $\mathcal{S}$, $\mathcal{N}$, k, η]
− $\mathcal{I}^{\mathrm{ex}}_{i,j}$[$\lambda$, $\mathcal{S}$, $\mathcal{N}$, k, η], {i, 0, $\mathcal{N}-1$}, {j, 0, $\mathcal{N}-1$}]]

In[10] := **$\mathcal{B}$ /: $\mathcal{B}_{\mathcal{N}\_}$:= Function[{k, m}, Table[$\beta_{i,j}$[k, |m|], {i, 0, $\mathcal{N}-1$}, {j, 0, $\mathcal{N}-1$}]]**

The kinetic energy integrals are defined by

$$\alpha_{ij} = \int_0^\infty \left(\frac{1}{2} v'^*_{i,m^\lambda}(r) v'_{j,m^\lambda}(r) + \frac{(m^\lambda)^2}{2r^2} v^*_{i,m^\lambda}(r) v_{j,m^\lambda}(r)\right) r\,\mathrm{d}r. \tag{21}$$

The required integrals are evaluated in Appendix B using the properties of the generalized Laguerre polynomials [14], and the results are implemented as the elements of a tridiagonal matrix.

$$In[11] := \boldsymbol{\alpha_{i\_,j\_}[k\_, m\_] /; j > i = \frac{(i+m+1)!\delta_{i+1,j}}{4k^m i!}};$$

$$In[12] := \boldsymbol{\alpha_{i\_,j\_}[k\_, m\_] /; i > j = \alpha_{j,i}[k, m]};$$

$$In[13] := \boldsymbol{\alpha_{i\_,i\_}[k\_, m\_] = \frac{(2i+m+1)(i+m)!}{4k^m i!}};$$

The overlap integrals are defined by

$$\beta_{ij} = \int_0^\infty v^*_{i,m^\lambda}(r) v_{j,m^\lambda}(r) r \, \mathrm{d}r, \tag{22}$$

which, again, can be evaluated analytically using the orthogonality relationship of the generalized Laguerre polynomials [14] (see Appendix B for details).

$$In[14] := \boldsymbol{\beta_{i\_,i\_}[k\_, m\_] = \frac{1}{2k^{m+1}} \frac{(i+m)!}{i!}};$$

$$In[15] := \boldsymbol{\beta_{i\_,j\_}[k\_, m\_] = 0};$$

This definition also allows us to write the normalization condition as,

$$\sum_{i=0}^{\mathcal{N}-1} \sum_{j=0}^{\mathcal{N}-1} c^*_{i,m^\lambda} \beta_{i,j} c_{j,m^\lambda} = 1 \Leftrightarrow \boldsymbol{c}^\dagger \mathcal{B} \boldsymbol{c} = 1. \tag{23}$$

The confining potential integrals are defined by

$$\mathcal{V}_{ij} = \int_0^\infty v^*_{i,m^\lambda}(r) V(r) v_{j,m^\lambda}(r) r \, \mathrm{d}r. \tag{24}$$

The integrals are easily evaluated for the harmonic confining potential, $V(r) = -V_0 + \frac{1}{2}k^2 r^2$ using the results already obtained from the calculation of the kinetic energy and overlap integrals (see Appendix B). The result is implemented as follows.

$$In[16] := \boldsymbol{\mathcal{V} /: \mathcal{V}_{i\_,j\_} := \mathcal{V} /: \mathcal{V}_{i,j} = \mathcal{V} /: \mathcal{V}_{j,i}}$$

$$\boldsymbol{= \text{Function}\left[\{k, V0, m\}, \text{Evaluate}\left[\frac{1}{4k^m i!}\left(\left((2i+m+1) - \frac{2V0}{k}\right)(i+m)!\delta_{i,j} - i(i+m)!\delta_{i-1,j} - (i+m+1)!\delta_{i+1,j}\right)\right]\right]}$$

Note that the inclusion of the symmetry requirement, $\mathcal{V}_{ij} = \mathcal{V}_{ji}$, through the use of dynamic programming increases efficiency.

The method is easily extended to different confining potentials. For example, in Appendix C we give an analytic solution for a *Gaussian confining potential*, and integrals for other more complicated potentials may be performed numerically.

The direct integrals defined by

$$\mathcal{I}^d_{ij} = \int_0^\infty \mathcal{V}^d_\lambda(r) v^*_{i,m^\lambda}(r) v_{j,m^\lambda}(r) r \, \mathrm{d}r = \frac{1}{2} \sum_{\mu \neq \lambda} \sum_{p=0}^{\mathcal{N}-1} \sum_{q=0}^{\mathcal{N}-1} c^*_{p,m^\mu} c_{q,m^\mu} k^{-m^\lambda - m^\mu - 3/2} \mathfrak{d}\big[\{i, j, m^\lambda\}, \{p, q, m^\mu\}\big],$$

can be implemented in *Mathematica* as

$$\begin{aligned}
&\textit{In[17]} := \mathcal{I}^{d}_{\mathbf{i_},\mathbf{j_}}[\boldsymbol{\lambda}_, \boldsymbol{\mathcal{S}}_, \boldsymbol{\mathcal{N}}_, \mathbf{k}_, \boldsymbol{\eta}_] \\
&\quad := \mathbf{Module}\Bigg[\{\sigma\}, \sigma = \mathbf{DeleteCases}[\boldsymbol{\mathcal{S}}, \boldsymbol{\lambda}]; \\
&\qquad \frac{1}{2}\sum_{\kappa=1}^{\mathbf{Length}[\sigma]}\sum_{p=1}^{\mathcal{N}}\sum_{q=1}^{\mathcal{N}} c_{\sigma[\![\kappa]\!],\eta}[\![p]\!]c_{\sigma[\![\kappa]\!],\eta}[\![q]\!]k^{-|\lambda[\![2]\!]|-|\sigma[\![\kappa,2]\!]|-3/2}\mathfrak{d}\big[\{i, j, |\lambda[\![2]\!]|\}, \{p-1, q-1, |\sigma[\![\kappa, 2]\!]|\}\big]\Bigg]
\end{aligned}$$

where

$$\begin{aligned}
&\mathfrak{d}\big[\{i, j, m^{\lambda}\}, \{p, q, m^{\mu}\}\big] \\
&\quad = 2k^{m^{\lambda}+m^{\mu}+3/2}\int_0^{\infty} v^{*}_{i,m^{\lambda}}(r)v_{j,m^{\lambda}}(r)\int_0^{\infty} v^{*}_{p,m^{\mu}}(r\xi)v_{q,m^{\mu}}(r\xi)\frac{\mathcal{V}_0(\xi)}{|1-\xi|}r\xi\,\mathrm{d}\xi r\,\mathrm{d}r. \qquad (25)
\end{aligned}$$

The exchange integrals defined by

$$\begin{aligned}
\mathcal{I}^{\mathrm{ex}}_{ij} &= \int_0^{\infty} v^{*}_{i,m^{\lambda}}(r)\mathcal{V}^{\mathrm{ex}}_{\lambda}(r)v_{j,m^{\lambda}}(r)r\,\mathrm{d}r \\
&= \frac{1}{2}\sum_{\mu\neq\lambda}\sum_{p=0}^{\mathcal{N}-1}\sum_{q=0}^{\mathcal{N}-1} c^{*}_{p,m^{\mu}}c_{q,m^{\mu}}\delta_{m^{\mu}_S,m^{\lambda}_S}k^{-m^{\lambda}-m^{\mu}-3/2}\mathfrak{f}\big[\{i, j, m^{\lambda}\}, \{p, q, m^{\mu}\}\big],
\end{aligned}$$

can be implemented in *Mathematica* as

$$\begin{aligned}
&\textit{In[18]} := \mathcal{I}^{\mathbf{ex}}_{\mathbf{i_},\mathbf{j_}}[\boldsymbol{\lambda}_, \boldsymbol{\mathcal{S}}_, \boldsymbol{\mathcal{N}}_, \mathbf{k}_, \boldsymbol{\eta}_] \\
&\quad := \mathbf{Module}\Bigg[\{\sigma\}, \sigma = \mathbf{DeleteCases}\big[\mathbf{DeleteCases}[\boldsymbol{\mathcal{S}}, \boldsymbol{\lambda}], \{_, _, -\boldsymbol{\lambda}[\![3]\!]\}\big]; \\
&\qquad \frac{1}{2}\sum_{\kappa=1}^{\mathbf{Length}[\sigma]}\sum_{p=1}^{\mathcal{N}}\sum_{q=1}^{\mathcal{N}} c_{\sigma[\![\kappa]\!],\eta}[\![p]\!]c_{\sigma[\![\kappa]\!],\eta}[\![q]\!]k^{-|\lambda[\![2]\!]|-|\sigma[\![\kappa,2]\!]|-3/2}\mathfrak{f}\big[\{i, j, |\lambda[\![2]\!]|\}, \{p-1, q-1, \sigma[\![\kappa, 2]\!]\}\big]\Bigg]
\end{aligned}$$

where

$$\begin{aligned}
&\mathfrak{f}\big[\{i, j, m^{\lambda}\}, \{p, q, m^{\mu}\}\big] \\
&\quad = 2k^{m^{\lambda}+m^{\mu}+3/2}\int_0^{\infty} v^{*}_{i,m^{\lambda}}(r)v_{p,m^{\mu}}(r)\int_0^{\infty} v^{*}_{q,m^{\mu}}(r\xi)v_{j,m^{\lambda}}(r\xi)\frac{\mathcal{V}_m(\xi)}{|1-\xi|}r\xi\,\mathrm{d}\xi r\,\mathrm{d}r. \qquad (26)
\end{aligned}$$

with $m = m^{\lambda} - m^{\mu} \in \mathbb{Z}$.

It is the calculation of these $\mathfrak{d}$ and $\mathfrak{f}$ integrals given by Eqs. (25) and (26), which is the most time consuming aspect of the procedure. In both cases we allow *Mathematica* to perform the integrations over r analytically, and then over ξ numerically, with *Mathematica*'s numerical integrator, **NIntegrate**, allowing for the singularity at $\xi = 1$.

The details are tedious, and are left for Appendix A. The required code is presented below. (Note the use of dynamic programming, which increases efficiency by including all necessary symmetries.) To speed up the computation, the analytic expressions could be exported as Fortran or C code and then integrated numerically using a suitable quadrature routine.

$$
\begin{aligned}
In[19] :=\ & \mathfrak{d}\big[\{\mathbf{i}_-, \mathbf{j}_-, \mathbf{m}_-\}, \{\mathbf{p}_-, \mathbf{q}_-, \mathbf{n}_-\}\big] \\
:=\ & \mathfrak{d}\big[\{i,j,m\},\{p,q,n\}\big] = \mathfrak{d}\big[\{i,j,m\},\{q,p,n\}\big] = \mathfrak{d}\big[\{j,i,m\},\{p,q,n\}\big] = \mathfrak{d}\big[\{j,i,m\},\{q,p,n\}\big] \\
=\ & \mathbf{NIntegrate}\left[\mathbf{Evaluate}\left[\frac{1}{2\pi}\xi^{2n+1}\frac{\mathfrak{V}_0[\xi]}{|1-\xi|}\langle\{i,j\},\{p,q\},1\rangle[m,n,\xi]\right],\{\xi,0,1,\infty\}\right] \\
In[20] :=\ & \mathfrak{f}\big[\{\mathbf{i}_-, \mathbf{j}_-, \mathbf{m}_-\}, \{\mathbf{p}_-, \mathbf{q}_-, \mathbf{n}_-\}\big] \\
:=\ & \mathfrak{f}\big[\{i,j,m\},\{p,q,n\}\big] = \mathfrak{f}\big[\{p,q,n\},\{i,j,m\}\big] = \mathfrak{f}\big[\{i,j,-m\},\{p,q,-n\}\big] = \mathfrak{f}\big[\{p,q,-n\},\{i,j,-m\}\big] \\
=\ & \mathbf{NIntegrate}\left[\mathbf{Evaluate}\left[\frac{1}{2\pi}\xi^{2|n|+1}\frac{\mathfrak{V}_{|m-n|}[\xi]}{|1-\xi|}\langle\{i,j\},\{p,q\},2\rangle[|m|,|n|,\xi]\right],\{\xi,0,1,\infty\}\right]
\end{aligned}
$$

$\langle\{i,j\},\{p,q\},1\rangle$ and $\langle\{i,j\},\{p,q\},2\rangle$ are defined by

$$
\begin{aligned}
In[21] :=\ & \big\langle\{\mathbf{i}_-, \mathbf{j}_-\}, \{\mathbf{p}_-, \mathbf{q}_-\}, 1\big\rangle \\
:=\ & \big\langle\{i,j\},\{p,q\},1\big\rangle = \big\langle\{j,i\},\{p,q\},1\big\rangle = \big\langle\{i,j\},\{q,p\},1\big\rangle = \big\langle\{j,i\},\{q,p\},1\big\rangle \\
=\ & \mathbf{Function}\big[\{m,n,\xi\},\mathbf{Evaluate}\big[(1+\xi^2)^{-m-n-3/2}\mathbf{Collect}[\mathbf{Expand}[x^a r^b L_p^n(x)L_q^n(x)L_i^m(r)L_j^m(r)], \\
& \qquad \{x^{(\_:1)}r^{(\_:1)}\},\mathbf{Simplify}]\,/.\,\mathbf{c}_-.x^{a+\eta_-\cdot}r^{b+\mathbf{l}_-\cdot} :\to c\mathcal{I}_{l,\eta,m,n}[\xi]\big]\big] \\
In[22] :=\ & \big\langle\{\mathbf{i}_-, \mathbf{j}_-\}, \{\mathbf{p}_-, \mathbf{q}_-\}, 2\big\rangle \\
:=\ & \big\langle\{i,j\},\{p,q\},2\big\rangle = \big\langle\{j,i\},\{p,q\},2\big\rangle = \big\langle\{i,j\},\{q,p\},2\big\rangle = \big\langle\{j,i\},\{q,p\},2\big\rangle \\
=\ & \mathbf{Function}\big[\{m,n,\xi\},\mathbf{Evaluate}\big[(1+\xi^2)^{-m-n-3/2}\mathbf{Collect}[\mathbf{Expand}[x^a r^b L_p^n(r)L_q^n(x)L_i^m(r)L_j^m(x)], \\
& \qquad \{x^{(\_:1)}r^{(\_:1)}\},\mathbf{Simplify}]\,/.\,\mathbf{c}_-.x^{a+\eta_-\cdot}r^{b+\mathbf{l}_-\cdot} :\to c\mathcal{I}_{l,\eta,m,n}[\xi]\big]\big]
\end{aligned}
$$

where

$$
In[23] := \mathcal{I}\,/\!:\mathcal{I}_{\mathbf{l}_-,\eta_-,\mathbf{m}_-,\mathbf{n}_-} := \mathbf{Function}\big[\{\xi\},\xi^{2\eta}(1+\xi^2)^{-l-\eta}\Gamma\big(m+n+l+\eta+\tfrac{3}{2}\big)\big]
$$

3.4. Total energy calculation

The total energy $\mathcal{E}$ of the system is given by

$$
\mathcal{E}[\Psi] = \langle\Psi|\mathcal{H}|\Psi\rangle = \langle\Psi|\mathcal{H}_1|\Psi\rangle + \langle\Psi|\mathcal{H}_2|\Psi\rangle.
$$

Note that this is *not* just the sum of the individual electron energies $\mathcal{E}_\lambda$, because the sum over all $\mathcal{E}_\lambda$ counts the kinetic energy and interaction energy with the confining potential once, while the mutual interaction energy is counted twice. Hence, the total energy can also be written as

$$
\mathcal{E}[\Psi] = \sum_\lambda \mathcal{E}_\lambda - \langle\Psi|\mathcal{H}_2|\Psi\rangle. \tag{27}
$$

Using the fact that $\mathcal{H}_2$ is of the form of a two electron operator, it can be shown (Appendix A) that

$$
\begin{aligned}
\langle\Psi|\mathcal{H}_2|\Psi\rangle = \frac{1}{2}\sum_{\lambda>\mu}\Bigg(\sum_{i,j,p,q=0}^{\mathcal{N}-1} & c_{i,m^\lambda}c_{j,m^\lambda}c_{p,m^\mu}c_{q,m^\mu} \\
& \cdot k^{-m^\lambda-m^\mu-3/2}\big(\mathfrak{d}[\{i,j,m^\lambda\},\{p,q,m^\mu\}] - \delta_{m_S^\lambda,m_S^\mu}\mathfrak{f}[\{i,j,m^\lambda\},\{p,q,m^\mu\}]\big)\Bigg),
\end{aligned} \tag{28}
$$

with $\mathfrak{d}$ and $\mathfrak{f}$ defined as in Eqs. (25) and (26).

The total energy is computed directly as follows.

```
In[24] := ℰ[𝒮_, 𝒩_, k_, η_] := ℰ[𝒮, 𝒩, k, η]
  = Sum[ℰ_{𝒮[[λ]],η}, {λ, 1, Length[𝒮]}]
    - 1/2 Sum[Sum[Sum[Sum[Sum[Sum[c_{𝒮[[λ]],η}[[i]] c_{𝒮[[λ]],η}[[j]] c_{𝒮[[μ]],η}[[p]] c_{𝒮[[μ]],η}[[q]]
      · (k^(-|𝒮[[λ,2]]|-|𝒮[[μ,2]]|-3/2) 𝔡({i-1, j-1, |𝒮[[λ, 2]]|}, {p-1, q-1, |𝒮[[μ, 2]]|})
        - δ_{𝒮[[λ,3]],𝒮[[μ,3]]} k^(-|𝒮[[λ,2]]|-|𝒮[[μ,2]]|-3/2) 𝔣({i-1, j-1, |𝒮[[λ, 2]]|}, {p-1, q-1, |𝒮[[μ, 2]]|}))
      , {q, 1, 𝒩}], {p, 1, 𝒩}], {j, 1, 𝒩}], {i, 1, 𝒩}], {μ, 1, λ-1}], {λ, 1, Length[𝒮]}]
```

3.5. Hartree–Fock evaluation

The module **HartreeFock** is the main program body for running the Hartree–Fock calculation to solve for N electrons defined by the state list $\mathcal{S}$ (see the examples section for a detailed explanation) with a matrix (expansion) size $\mathcal{N}$. Self-consistency is obtained by setting up a while loop which runs until the energy difference between two consecutive iterations is less than δ. The parameters k and V_0 define the confining potential (e.g., the harmonic confining potential of the form $V(r) = -V_0 + \frac{1}{2}k^2r^2$).

```
In[25] := HartreeFock[𝒮_, 𝒩_, δ_, k_, V0_]
  := Module[{𝒟 = 2δ, η = 0, τ1 = 0, τ2 = 0},
    τ1 = First[Timing[
      InitialiseMatrixElements[𝒩]; ]];
    τ2 = First[Timing[
      InitialiseCoefficients[𝒮, 𝒩, k];
      StateSolve[𝒮, 𝒩, k, V0, η];
      While[Abs[𝒟] > δ,
        η++;
        StateSolve[𝒮, 𝒩, k, V0, η];
        𝒟 = ℰ[𝒮, 𝒩, k, η+1] - ℰ[𝒮, 𝒩, k, η]
      ]
    ]];
    SaveIntegrals;
    PrintOutput[𝒮, 𝒟, η];
    Print["Initialization Time = ", τ1];
    Print["Running Time = ", τ2]
  ]
```

InitialiseMatrixElements is used to help save time with future calculations. All the **AngleBracket** function definitions (*ie*, $\langle\{i, j\}, \{p, q\}, 1\rangle$ and $\langle\{i, j\}, \{p, q\}, 2\rangle$) required for an $\mathcal{N} \times \mathcal{N}$ matrix expansion are saved in a file called *matrix*$\mathcal{N}$*.mx* in a subdirectory of the home directory called *HFData*. This module creates the file and subdirectory if they do not already exist, and loads the file otherwise. It also loads values for the integrals $\mathfrak{d}$ and $\mathfrak{f}$ if they have been saved in the files *d.mx* and *f.mx*.

```
In[26] := InitialiseMatrixElements[𝒩_]
    := Module[{},
        SetDirectory[$HomeDirectory];
        If[FileNames["HFData"] == {}, CreateDirectory["HFData"]];
        If[FileNames[ToFileName["HFData″, "matrix" <> ToString[𝒩] <> ".mx"]] == {},
          Table[⟨{i, j}, {p, q}, 1⟩, {i, 0, 𝒩 − 1}, {j, 0, 𝒩 − 1}, {p, 0, 𝒩 − 1}, {q, 0, 𝒩 − 1}];
          Table[⟨{i, j}, {p, q}, 2⟩, {i, 0, 𝒩 − 1}, {j, 0, 𝒩 − 1}, {p, 0, 𝒩 − 1}, {q, 0, 𝒩 − 1}];
          DumpSave[ToFileName["HFData", "matrix" <> ToString[𝒩] <> ".mx"], AngleBracket],
          Get[ToFileName["HFData", "matrix" <> ToString[𝒩] <> ".mx"]]];
        If[FileNames[ToFileName["HFData", "d.mx"]] ≠ {},
          Get[ToFileName["HFData", "d.mx"]]];
        If[FileNames[ToFileName["HFData", "f.mx"]] ≠ {},
          Get[ToFileName["HFData", "f.mx"]]];
    ]
```

InitialiseCoefficients assigns initial values to the expansion coefficients, and uses **NormaliseCoefficients** to normalize them so that $c^{\dagger}\mathcal{B}c = 1$ (Eq. (23)).

```
In[27] := InitialiseCoefficients[𝒮_, 𝒩_, k_]
    := Module[{χ, m, n}
        χ = Table[0, {j, 𝒩}];
        Do[n = 𝒮[[i]][[1]]; m = 𝒮[[i]][[2]];
          c /: c_{𝒮[[i]],0} = NormaliseCoefficients[ReplacePart[χ, 1, n + 1], k, m];
          , {i, Length[𝒮]}]
    ]
```

$$\text{In[28]} := \text{NormaliseCoefficients[c\_List, k\_, m\_]} := \frac{c}{\sqrt{c.\mathcal{B}_{\text{Length}[c]}[k, m].c}};$$

StateSolve solves the Rayleigh–Ritz matrix equation, Eq. (8) for each electron in the system, and then assigns a new set of normalized coefficients based on the solutions.

```
In[29] := StateSolve[𝒮_, 𝒩_, k_, V0_, η_]
  := Module[{λ, ε, χ},
    Do[λ = 𝒮[[i]];
      {ε, χ} = Transpose[Select[(Chop[Eigensystem[(ℬ𝒩[k, λ[[2]]])^-1.𝒜𝒩[λ, 𝒮, k, V0, η] // N]])^T,
                                First[#1] < 0&]];
      c /: c_{λ,η+1} = Part[NormaliseCoefficients[#1, k, λ[[2]]]&/@χ, λ[[1]] + 1];
      ℰ /: ℰ_{λ,η+1} = ε[[λ[[1]] + 1]];
      , {i, Length[𝒮]}]
  ]
```

Upon exiting the self-consistency loop, we save the values for the $\mathfrak{d}$ and $\mathfrak{f}$ integrals using the **SaveIntegrals** module (they are saved to the files *d.mx* and *f.mx* in the *HFData* subdirectory of the home directory). This is done to increase efficiency in further calculations of different electronic configurations for the same potential, since it is not necessary to reevaluate these time consuming integrals.

```
In[30] := SaveIntegrals
       := Module[{},
            DumpSave[ToFileName["HFData", "d.mx"], 𝔡];
            DumpSave[ToFileName["HFData", "f.mx"], 𝔣];
            ResetDirectory[];
          ]
```

PrintOutput is a module which can be modified by the user depending upon the desired output. In this example, the calculated energies (converted to meV) are saved under the symbol $\mathfrak{E}$, and the expansion coefficients under the symbol $\mathfrak{C}$. The total energy, number of iterations, and the energy difference between the last two iterations are printed out. By default, the conversion factors are those of GaAs, which has an effective mass $m^* = 0.065m_e$ and dielectric constant $\epsilon = 12.9\epsilon_0$.

```
In[31] := PrintOutput[𝒮_, 𝒟_, η_]
       := Module[{Hartree = 27.2116, ϵ = 12.9, m = 0.065},
            Do[𝔈 /: 𝔈Length[𝒮],𝒮[[i]] = 1000 m Hartree/ϵ^2 ℰ𝒮[[i]],η+1;
               𝔈 /: 𝔈Length[𝒮],𝒮[[i]] = c𝒮[[i]],η+1,
               {i, Length[𝒮]}];
            𝔈 /: 𝔈Length[𝒮] = 1000 m Hartree/ϵ^2 ℰ[𝒮, 𝒩, k, η + 1];
            Print["Total Energy = ", 𝔈Length[𝒮], "meV"];
            Print["Number of Iterations = ", η + 1];
            Print["Convergence = ", 1000 m Hartree/ϵ^2 𝒟]
          ]
```

To give an idea of the time required for the calculations, the initialization time and the time required to complete the Hartree–Fock self-consistency loop are also printed out.

4. Examples and results

In this section we start by explaining the filling order of these quantum dots. This helps explain the data structure for the state list $\mathcal{S}$. We give an example for both a three- and two-electron GaAs quantum dot system, and then go on to describe some of the results obtained using the **QDHartreeFock.m** package.

$\mathcal{E}$	k	$2k$	$2k$	$3k$	$3k$	$3k$	
N	$\{0,0\}$	$\{0,1\}$	$\{0,-1\}$	$\{0,2\}$	$\{0,-2\}$	$\{1,0\}$	
1	↑						
2	↑↓						**
3	↑↓	↑					
4	↑↓	↑	↑				*
5	↑↓	↑↓	↑				
6	↑↓	↑↓	↑↓				**
7	↑↓	↑↓	↑↓	↑			
8	↑↓	↑↓	↑↓	↑	↑		
9	↑↓	↑↓	↑↓	↑	↑	↑	*
10	↑↓	↑↓	↑↓	↑↓	↑	↑	
11	↑↓	↑↓	↑↓	↑↓	↑↓	↑	
12	↑↓	↑↓	↑↓	↑↓	↑↓	↑↓	**

Fig. 2. Filling order for a two-dimensional system. The top row gives the single electron eigenenergies for the harmonic confining potential ($V_0 = 0$) for the states $\{n, m\}$. We have labeled the full-shells by (**), and the half-filled shells by (*).

4.1. Filling order

We recall that the energy eigenvalues for a single electron in a two-dimensional harmonic oscillator potential is given by Eq. (3), so that

$$\mathcal{E}_{n,|m|} = k\big(2n + |m| + 1\big) - V_0.$$

Assuming that these energy levels hold for systems with more electrons, and then applying Hund's rules [15], we get the filling order described by Fig. 2. We can see that there are full-shells for $N = 2, 6, 12, \ldots$ and half-filled shells for $N = 4, 9, 16, \ldots$. In an atomic systems these "magic numbers" would correspond to peaks in the addition energy of these elements, with full-shells corresponding to larger peaks than the half-filled shells.

4.2. Example

The first step is to load in the package. This can be done either by opening the **QDHartreeFock.nb** file and evaluating the initialization cells (using the menu: *Kernel* | *Evaluation* | *Evaluate Initialisation*), or by loading in the **QDHartreeFock.m** package. The latter can be done by first saving the package in a directory inside the *ExtraPackages* directory in the *Mathematica* folder, and then using <<. For example,

```
<< QDHartreeFock`
```

We now assign values to the parameters k and V_0 in the harmonic confining potential of the form $V(r) = -V_0 + \frac{1}{2}k^2r^2$, say $k = 10$ and $V_0 = 100$.

```
In[32] := k = 10.0; V0 = 100.0;
```

Consider the lowest energy states of the 2- and 3-electron systems according to the filling order in Fig. 2, $\mathcal{S}\mathbf{2}$ and $\mathcal{S}\mathbf{3}$ are defined by listing the states $\{n, m, m_S\}$ of each electron,

```
In[33] := S2 = {{0, 0, 1/2}, {0, 0, -1/2}};
```

In[34] := $\mathcal{S}\mathbf{3} = \{\{0, 0, \frac{1}{2}\}, \{0, 0, -\frac{1}{2}\}, \{0, 1, \frac{1}{2}\}\}$;

We set the following parameters which determine the accuracy of the calculation: a matrix (expansion) size of, say $\mathcal{N} = 4$, and a value for δ, the energy difference between the last two iterations, of, say $\delta = 10^{-7}$.

In[35] := $\mathcal{N} = 4;\ \delta = 10^{-7}$

We can now run the Hartree–Fock calculations. For the 3-electron system,

In[36] := **HartreeFock[**$\mathcal{S}\mathbf{3}, \mathcal{N}, \delta, k, \mathbf{V_0}$**]**

Total Energy $= -2673.07$ meV

Number of Iterations $= 9$

Convergence $= 8.38467 \times 10^{-7}$

Initialisation Time $= 185.749$ second

Running Time $= 479.86$ second

For the 2-electron system,

In[37] := **HartreeFock[**$\mathcal{S}\mathbf{2}, \mathcal{N}, \delta, k, \mathbf{V_0}$**]**

Total Energy $= -1872.15$ meV

Number of Iterations $= 9$

Convergence $= 1.97748 \times 10^{-7}$

Initialisation Time $= 1.74997$ second

Running Time $= 4.9083$ second

Notice the significant time saving in both the initialization time and the running time for the solution of the $\mathcal{S}\mathbf{2}$ state once the $\mathcal{S}\mathbf{3}$ state has been solved for. This is due to the fact that many of the time consuming aspects of the code are saved after the first time **HartreeFock** is run.

Implementation of this procedure was performed with *Mathematica* version 4.1, running remotely from a DEC Alpha workstation 500 with 0.5 GB RAM. Convergence was obtainable, with δ becoming less than 10^{-7} for anywhere between 4 and 20 iterations depending on the number of electrons in the system.

Calculations were performed for quantum dots with up to $N = 18$ electrons. As would be expected, calculation time increased with each extra electron, markedly so when jumping to a higher energy level. The program is limited in that calculations with matrix (expansion) sizes larger than $\mathcal{N} = 4$ become laborious due to increased running times and CPU load. This limitation on the expansion means a deficiency in the accuracy of the calculations, especially as the electron number increases. It also means that calculations with non-harmonic confining potentials are not feasible for more than one electron with the present code. The limitation is caused by the time required to calculate the $\mathfrak{d}$ and $\mathfrak{f}$ terms (see §3.3).

4.3. Addition energy

Due to Coulomb repulsion, the energy of a quantum dot with $N + 1$ electrons is greater than the energy of a dot with N electrons. Thus the addition of an electron requires energy to be supplied. The chemical potential is defined as $\mu(N) \equiv E(N) - E(N-1)$ with $E(N)$ being the ground state energy for the N-electron system. The capacitative, or addition energy is then

$$\Delta\mu(N) = \mu(N+1) - \mu(N) = E(N+1) - 2E(N) + E(N-1).$$

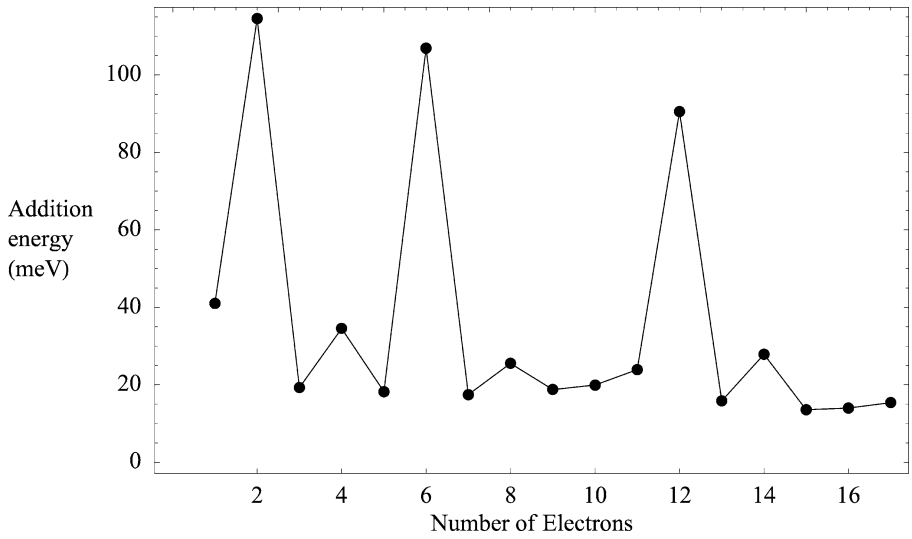

Fig. 3. Addition energies calculated by the Hartree–Fock method with $\mathcal{N} = 4$ and $k = 10$.

We can use this definition to plot the addition energies obtained from our Hartree–Fock calculations (Fig. 3). From a comparison with the filling order (Fig. 2), we immediately see the expected peaks with 2, 6, and 12 electrons. We also obtain the smaller half-filling peak at $N = 4$. However, we notice that the expected small peaks for $N = 9$ and 16 are not seen. In fact it appears as though we obtained peaks at $N = 8$ and 14 instead. Possible reasons are discussed in §4.4.

Tarucha et al. [11] were able to experimentally measure the addition energy of a quantum dot structure (Fig. 4). As a negative voltage is applied to the side gate, the diameter of the dot becomes smaller and excess electrons are forced out one at a time until there are none left in the conduction band. A current will flow only if the number of electrons in the dot changes. As discussed in their paper, this will only happen when certain discrete energies are supplied, and so current peaks are observed at the corresponding voltages. The voltage difference between current peaks is a measure of the addition energy, and the experimental data indeed indicates the expected behaviour associated with a two-dimensional structure.

The experimental data of Tarucha et al. [11] and the theoretical results of Ezaki et al. [9] have energies within the 0–10 meV range, while our calculations for $k = 10$ range up to about 120 meV. In order to understand how the width and depth of the quantum dots affect the absolute scale of Fig. 3, we examined the effect of varying the parameter k (Fig. 5). We observe that as k is decreased, the addition energies are shifted down to lower energies. The peak positions appear to be unaffected, except for the fact that the main peaks become less pronounced. Below about $k = 1$, we lose the ability to identify the main peaks at $N = 2$ and 6. This trend agrees with the theoretical results obtained using density functional theory by Lee et al. [10] (Fig. 6). The overall agreement of the two results is very pleasing. Note that Lee et al. [10] also get a "bump" at $N = 8$ as well as a different energy range from the experimental data.

The observed trend can be explained by the fact that as k decreases, the well is becoming shallower. Thus, the effect of the quantum confinement becomes less pronounced and the interaction energies become increasingly important. The electrons start to show the behaviour of free particles.

Another thing we notice from a comparison with Fig. 4 is that the experimental peaks tend to fall off more rapidly than all three theoretical results. This is perhaps due to the fact that our calculations, and also those of Lee

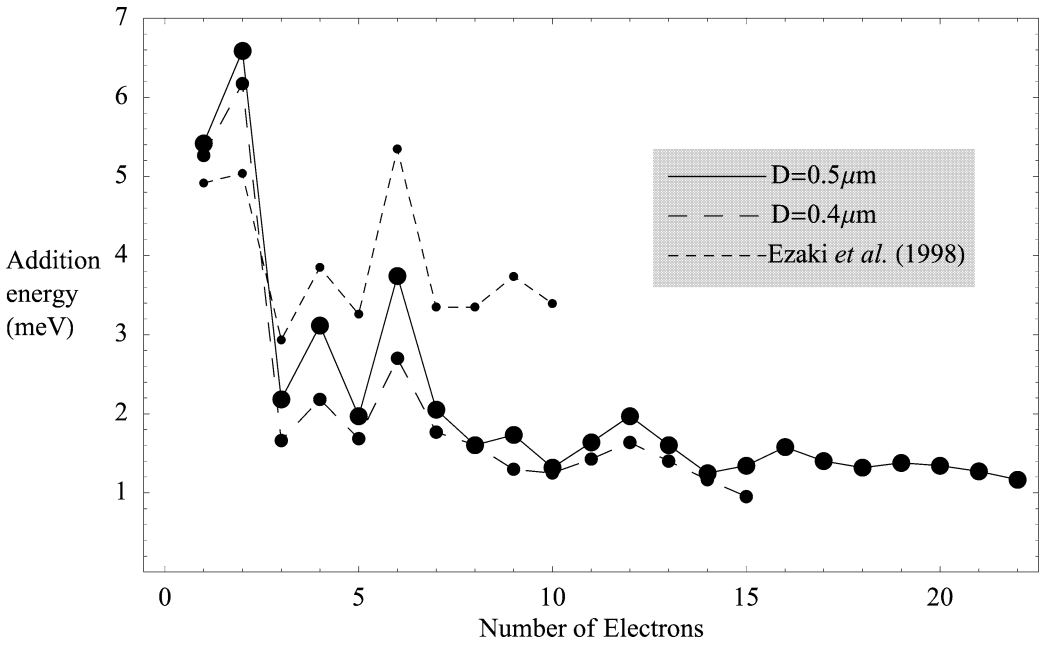

Fig. 4. Addition energies as measured by Tarucha et al. [11] for two different dot sizes of 0.5 and 0.4 μm. Also plotted are the theoretical results of Ezaki et al. [9].

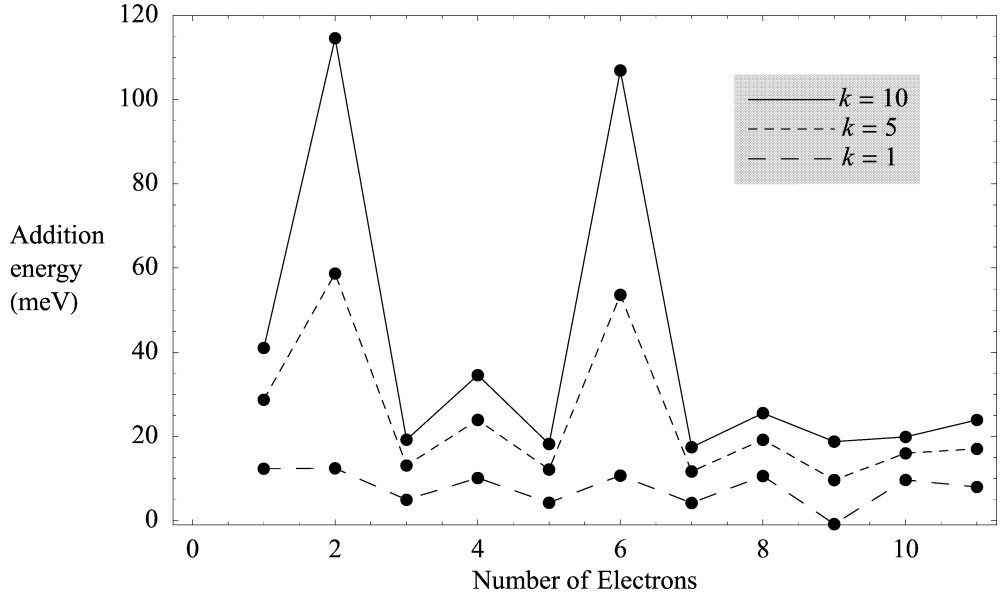

Fig. 5. Effect of varying the parameter k in the confining potential $V(r) = \frac{1}{2}k^2r^2$.

et al. [10], are performed for fixed k, whereas the experimental technique of slowly altering the voltage to remove the electrons would scan through a range of k values.

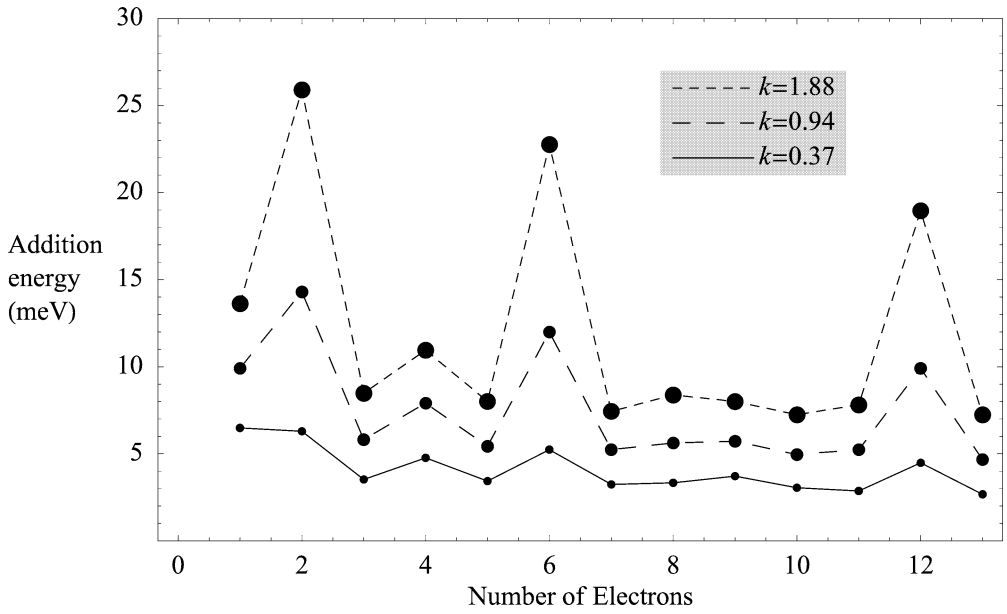

Fig. 6. Theoretical results of Lee et al. [10] calculated using density functional theory. Their values for $\hbar\omega = 4$, 10, 20 meV, correspond to $k = 0.37$, 0.94, 1.88.

4.4. Possible reasons for peak at $N = 8$

Firstly, note that the filling order is ambiguous. For example, the two different filling orders,

N	$\{0,0\}$	$\{0,1\}$	$\{0,-1\}$	$\{0,2\}$	$\{0,-2\}$	$\{1,0\}$
8	$\uparrow\downarrow$	$\uparrow\downarrow$	$\uparrow\downarrow$	$\uparrow$	$\uparrow$	

and

N	$\{0,0\}$	$\{0,1\}$	$\{0,-1\}$	$\{0,2\}$	$\{0,-2\}$	$\{1,0\}$
8	$\uparrow\downarrow$	$\uparrow\downarrow$	$\uparrow\downarrow$	$\uparrow$		$\uparrow$

are almost degenerate. Choosing one or the other can alter where we observe the "peak". It is possible that the actual result should have contributions from both.

Secondly, the Hartree–Fock approximation assumes that each electron moves independently in a mean field determined by the other electrons. This assumption ignores the effect of electron correlations. The correlation energy is defined as

$$\mathcal{E}^{\text{corr}} = \mathcal{E}^{\text{exact}} - \mathcal{E}^{\text{HF}}$$

Pfannkuche et al. [8] showed that correlation was important in their comparison of an exact solution and a Hartree–Fock solution for artificial helium. Their results were in good agreement for the triplet state calculations, but were not so for the singlet state. This was due to the exact singlet states containing products of one-particle states with different angular momenta—something not accounted for in the Hartree–Fock solutions.

Both the lack of correlations and the degeneracy of filling orders can be corrected for by using a *multi-configuration Hartree–Fock* (MCHF) approach [18]. When dealing with atomic systems we can consider linear combinations of Slater determinants with the same n and l quantum numbers but different m_l and m_S called configuration state functions (CSF). These are denoted $\Phi(\gamma L M_L S M_S)$, and are better approximations to the total wavefunction than the single Slater determinant. Better approximations can be made with linear combinations of CSF,

$$\Psi(\gamma LS) = \sum_{i=1}^{M} c_i \Phi(\gamma_i LS), \quad \text{where } \sum_{i=1}^{M} |c_i|^2 = 1.$$

These functions are the basis of the MCHF method, just as the Slater determinant was the basis for the Hartree–Fock method. These functions allow for variation in the angular momentum quantum numbers, which is expected to fix the problem of degenerate filling orders. Moreover, these functions have the advantage that they can take into account correlations.

4.5. *Exchange effect*

To demonstrate the importance of exchange interactions, we also performed calculations based on the original method of Hartree. In this method, the wavefunction is no longer a Slater determinant, but instead is a simple product of single electron wavefunctions. The effect of this is that we no longer have the exchange term in the Hartree–Fock equations; we are instead left with the Hartree equations, which for the ith electron in the state λ reads

$$\left(-\tfrac{1}{2}\nabla^2_{\boldsymbol{r}_i} + V(r_i) + \mathcal{V}^d_\lambda(\boldsymbol{r}_i)\right)\psi_\lambda(q_i) = \mathcal{E}_\lambda \psi_\lambda(q_i),$$

with $\mathcal{V}^d_\lambda$ defined as before. Also, since we no longer have a determinantal function, the total energy is now

$$\mathcal{E}[\Psi] = \sum_\lambda \mathcal{E}_\lambda - \langle \Psi | \mathcal{H}_2 | \Psi \rangle,$$

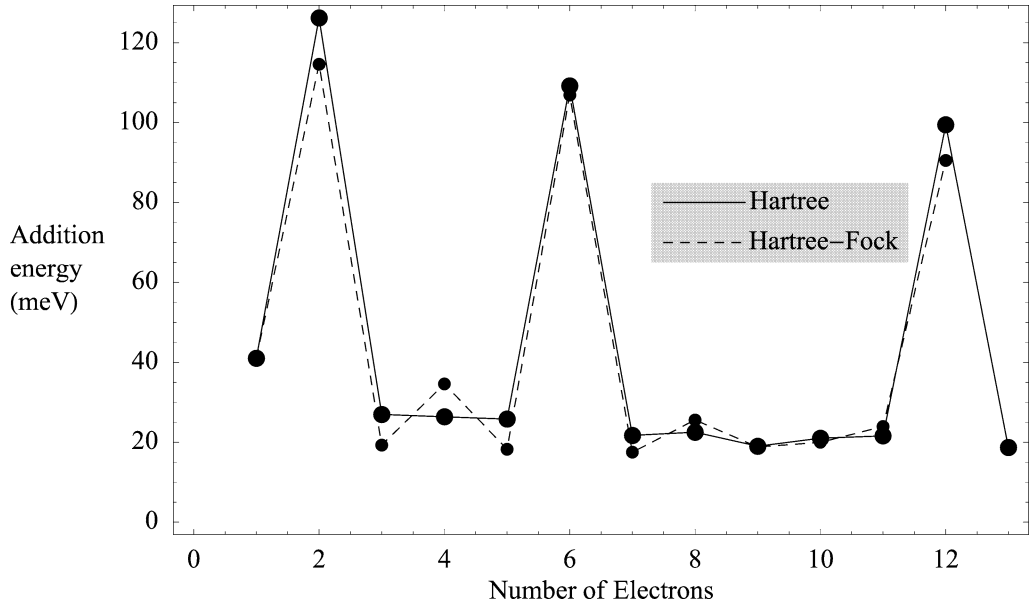

Fig. 7. Comparison of a Hartree and a Hartree–Fock calculation for $k = 10$.

with

$$\langle\Psi|\mathcal{H}_2|\Psi\rangle = \frac{1}{2}\sum_{\lambda>\mu}\left(\sum_{i=0}^{\mathcal{N}-1}\sum_{j=0}^{\mathcal{N}-1}\sum_{p=0}^{\mathcal{N}-1}\sum_{q=0}^{\mathcal{N}-1} c_{i,m^\lambda}c_{j,m^\lambda}c_{p,m^\mu}c_{q,m^\mu}k^{-m^\lambda-m^\mu-3/2}\mathfrak{d}\big[\{i,j,m^\lambda\},\{p,q,m^\mu\}\big]\right).$$

We performed a Hartree calculation for a value of $k = 10$ in the harmonic confining potential. The addition energy was plotted with the corresponding values from the Hartree–Fock calculations (Fig. 7). We can see that we lose the peaks due to the half-filling of states. This result was of course to be expected, since, without the effect of spin, there would not be any energy difference when we add electrons with parallel or antiparallel spins.

5. Conclusion

In this paper we have examined the electronic structure of circularly symmetric quantum dots with N-electrons. As a first step, we investigated the single electron solutions to the Schrödinger equation. A general method was developed which allows us to treat a wide range of different confining potentials. Analytic solutions for the eigenstates of a single electron in Gaussian confining potential were obtained.

A *Mathematica* package, **QDHartreeFock.nb** was developed which implements the Hartree–Fock method to solve quantum dot systems with N-electrons. The addition energies calculated in this manner are in good agreement with the theoretical work by Lee et al. [10]. The calculations also agree, at least at a qualitative level, with the experimental results of Tarucha et al. [11]. We also examined the exchange effect in an N-particle quantum dot—making a comparison between the Hartree and Hartree–Fock approximations.

In its present form, the code requires significant amount of CPU time and memory. A conversion of the code to a more numerical environment, such as Fortran or C, should speed up computation considerably. We will also look at revising the method to allow faster and more accurate calculation of the many multi-dimensional integrals involved in the Hartree–Fock formalism. A procedure based on solutions of pairs of differential equations is described by Fischer et al. [18], and may be adaptable to 2D quantum dot systems. Further research efforts will look towards anisotropic quantum dots, and the study of transport phenomena in quantum dot systems.

Acknowledgements

We would like to thank C. Hines and A.T. Stelbovics for helpful discussions.

Appendix A. Simplification for Hartree–Fock calculations

A.1. Simplification of Direct and Exchange potentials

Using the assumption from Eq. (14) and expanding r_{ij} as in Eq. (15) we can write the direct and exchange potentials, Eq. (12) as

$$\begin{aligned}\mathcal{V}_\lambda^d(\boldsymbol{r}_i) &= \sum_{\mu\neq\lambda}\int\frac{|\psi_\mu(\boldsymbol{r}_j)|^2}{r_{ij}}\,\mathrm{d}\boldsymbol{r}_j\\ &= \sum_{\mu\neq\lambda}\frac{1}{2\pi}\int_0^\infty\big|R_{n,m}(r_j)\big|^2\int_0^{2\pi}\frac{1}{r_>}\frac{1}{(1+\rho^2-2\rho\cos(\phi_j-\phi_i))^{1/2}}\,\mathrm{d}\phi\,r_j\,\mathrm{d}r_j,\end{aligned}$$

and the exchange potential, Eq. (13) as

$$\begin{aligned}\mathcal{V}_\lambda^{\mathrm{ex}}(\boldsymbol{r}_i)\psi_\lambda(\boldsymbol{r}_i) &= \sum_{\mu\neq\lambda}\delta_{m_S^\mu,m_S^\lambda}\psi_\mu(\boldsymbol{r}_i)\int\frac{\psi_\mu^*(\boldsymbol{r}_j)\psi_\lambda(\boldsymbol{r}_j)}{r_{ij}}\,\mathrm{d}\boldsymbol{r}_j\\ &= \sum_{\mu\neq\lambda}\delta_{m_S^\mu,m_S^\lambda}\frac{1}{2\pi}R_\mu^*(r_i)\mathrm{e}^{\mathrm{i}m^\mu\phi_i}\int_0^\infty R_\mu^*(r_j)R_\lambda(r_j)\\ &\quad\cdot\int_0^{2\pi}\frac{1}{r_>}\frac{\mathrm{e}^{\mathrm{i}m\phi_j}}{(1+\rho^2-2\rho\cos(\phi_j-\phi_i))^{1/2}}\,\mathrm{d}\phi_j r_j\,\mathrm{d}r_j,\end{aligned}$$

where $m=m^\lambda-m^\mu\in\mathbb{Z}$. Now

$$\begin{aligned}&\int_0^{2\pi}\frac{1}{r_>}\frac{\mathrm{e}^{\mathrm{i}m\phi_j}}{(1+\rho^2-2\rho\cos(\phi_j-\phi_i))^{1/2}}\,\mathrm{d}\phi_j\\ &\quad=\int_{-\phi_i}^{2\pi-\phi_i}\frac{1}{r_>}\frac{\mathrm{e}^{\mathrm{i}m(\phi_i+\phi_j)}}{(1+\rho^2-2\rho\cos(\phi_j))^{1/2}}\,\mathrm{d}\phi_j\\ &\quad=\mathrm{e}^{\mathrm{i}m\phi_i}\int_0^{2\pi}\frac{1}{r_>}\frac{\mathrm{e}^{\mathrm{i}m\phi_j}}{(1+\rho^2-2\rho\cos(\phi_j))^{1/2}}\,\mathrm{d}\phi_j\\ &\quad=\mathrm{e}^{\mathrm{i}m\phi_i}\int_0^{2\pi}\frac{1}{r_>}\frac{\cos(m\phi_j)}{(1+\rho^2-2\rho\cos(\phi_j))^{1/2}}\,\mathrm{d}\phi_j,\end{aligned}$$

where in the last step we have used symmetry arguments to drop the antisymmetric part of $\mathrm{e}^{\mathrm{i}m\phi}=\cos(m\phi)+\mathrm{i}\sin(m\phi)$. This integral can be evaluated for individual m, to give polynomials involving $K(x)$ and $E(x)$, the complete elliptic integrals of the first and second kinds, respectively [17]. We notice that if we change variables to $\xi=r_j/r_i$, then a factor of $1/|1-\xi|$ may be removed, and we are left with simplified forms of the direct and exchange potentials, given by Eqs. (17) and (18), where we have defined

$$\mathfrak{V}_m(\xi)=(1-\xi)\int_0^{2\pi}\frac{\cos(m\phi)}{(1+\xi^2-2\xi\cos(\phi))^{1/2}}\,\mathrm{d}\phi.$$

A.2. Matrix elements

We want to evaluate the integrals

$$\begin{aligned}&\mathfrak{d}\big[\{i,j,m^\lambda\},\{p,q,m^\mu\}\big]\\ &\quad=2k^{m^\lambda+m^\mu+3/2}\int_0^\infty v_{i,m^\lambda}^*(r)v_{j,m^\lambda}(r)\int_0^\infty v_{p,m^\mu}^*(r\xi)v_{q,m^\mu}(r\xi)\frac{\mathfrak{V}_0(\xi)}{|1-\xi|}r\xi\,\mathrm{d}\xi\,r\,\mathrm{d}r\\ &\quad=\int_0^\infty\xi^{2m^\mu+1}\frac{\mathfrak{V}_0(\xi)}{|1-\xi|}\big\langle\{i,j,m^\lambda\},\{p,q,m^\mu\},1\big\rangle\mathrm{d}\xi,\end{aligned}$$

and

$$
\begin{aligned}
&\mathfrak{f}\big[\{i,j,m^{\lambda}\},\{p,q,m^{\mu}\}\big]\\
&\quad= 2k^{m^{\lambda}+m^{\mu}+3/2}\int_0^{\infty} v^{*}_{i,m^{\lambda}}(r)v_{p,m^{\mu}}(r)\int_0^{\infty} v^{*}_{q,m^{\mu}}(r\xi)v_{j,m^{\lambda}}(r\xi)\frac{\mathfrak{V}_m(\xi)}{|1-\xi|}r\xi\,\mathrm{d}\xi\,r\,\mathrm{d}r\\
&\quad= \int_0^{\infty}\xi^{2m^{\mu}+1}\frac{\mathfrak{V}_m(\xi)}{|1-\xi|}\big\langle\{i,j,m^{\lambda}\},\{p,q,m^{\mu}\},2\big\rangle\mathrm{d}\xi,
\end{aligned}
$$

where we have defined

$$
\big\langle\{i,j,m\},\{p,q,n\},1\big\rangle = 2k^{m+n+3/2}\int_0^{\infty} r^{2m+2n+2}\mathrm{e}^{-kr^2}\mathrm{e}^{-kr^2\xi^2}L_p^n(kr^2\xi^2)L_q^n(kr^2\xi^2)L_i^m(kr^2)L_j^m(kr^2)\,\mathrm{d}r,
$$

and

$$
\big\langle\{i,j,m\},\{p,q,n\},2\big\rangle = 2k^{m+n+3/2}\int_0^{\infty} r^{2m+2n+2}\mathrm{e}^{-kr^2}\mathrm{e}^{-kr^2\xi^2}L_p^n(kr^2)L_q^n(kr^2\xi^2)L_i^m(kr^2)L_j^m(kr^2\xi^2)\,\mathrm{d}r,
$$

The generalized Laguerre polynomials in these integrals bring in certain powers of $kr^2\xi^2$ and kr^2, so we consider integrals of the form

$$
2k^{m+n+l+\eta+3/2}\int_0^{\infty} r^{2m+2n+2l+2\eta+2}\xi^{2\eta}\mathrm{e}^{-kr^2}\mathrm{e}^{-kr^2\xi^2}\,\mathrm{d}r
$$

which can be evaluated as

In[38] := **Clear[k]; SetOptions[Integrate, GenerateConditions → False];**

In[39] := $\mathbf{2k^{m+n+l+\eta+3/2}\int_0^{\infty} r^{2m+2n+2l+2\eta+2}\xi^{2\eta}e^{-kr^2}e^{-kr^2\xi^2}\,dr}$ **// Simplify // PowerExpand**

Out[39] $= \xi^{2\eta}(\xi^2+1)^{-l-m-n-\eta-3/2}\Gamma\big(l+m+n+\eta+\frac{3}{2}\big)$

From this we define the function, $\mathcal{I}_{l,\eta,m,n}$ from §3.3. We can then expand the generalized Laguerre polynomials, collect powers of $kr^2\xi^2$ and kr^2, and then match coefficients and use the above result to obtain the integrals $\langle\{i,j,m\},\{p,q,n\},1\rangle$ and $\langle\{i,j,m\},\{p,q,n\},2\rangle$. The remaining integration over r is performed numerically to obtain $\mathfrak{d}$ and $\mathfrak{f}$.

A.3. Total energy

For a two electron operator g_{ij} and a determinantal function Ψ, we can write [19]

$$
\left\langle\Psi\left|\sum_{i>j=1}^{N} g_{ij}\right|\Psi\right\rangle = \sum_{i>j=1}^{N}\big[\langle ij|g|ij\rangle - \langle ij|g|ji\rangle\big], \tag{A.1}
$$

where it is understood that in both the bra and the ket, the spin orbital written first is a function of q_1, and the second is a function of q_2. Eq. (27) gives the total energy as

$$
\mathcal{E}[\Psi] = \sum_{\lambda}\mathcal{E}_{\lambda} - \langle\Psi|\mathcal{H}_2|\Psi\rangle,
$$

where operator $\mathcal{H}_2$ is of the form of a two electron operator. So using the property from Eq. (A.1), we can write

$$\begin{aligned}\langle\Psi|\mathcal{H}_2|\Psi\rangle &= \sum_{\lambda>\mu}\Bigg(\iint \psi_\lambda^*(q_i)\psi_\mu^*(q_j)\mathcal{H}_2\psi_\lambda(q_i)\psi_\mu(q_j)\,\mathrm{d}q_j\,\mathrm{d}q_i \\ &\qquad - \iint \psi_\lambda^*(q_i)\psi_\mu^*(q_j)\mathcal{H}_2\psi_\lambda(q_j)\psi_\mu(q_i)\,\mathrm{d}q_j\,\mathrm{d}q_i\Bigg) \\ &= \sum_{\lambda\neq\mu}(\mathcal{I}_1+\mathcal{I}_2).\end{aligned}$$

Now, $\psi_\lambda(q)=\frac{1}{\sqrt{2\pi}}\mathrm{e}^{\mathrm{i}m^\lambda\phi}R_\lambda(r)\chi_{m_S^\lambda}$, so (using the orthonormality property of the spin functions χ) we can rewrite the above integrals as

$$\mathcal{I}_1=\frac{1}{4\pi^2}\int_0^\infty\int_0^\infty\int_0^{2\pi}\int_0^{2\pi} R_\lambda^*(r_i)R_\mu^*(r_j)\mathcal{H}_2R_\lambda(r_i)R_\mu(r_j)\,\mathrm{d}\phi_j\,\mathrm{d}\phi_i\,r_j\,\mathrm{d}r_j\,r_i\,\mathrm{d}r_i,$$

and

$$\mathcal{I}_2=\frac{1}{4\pi^2}\int_0^\infty\int_0^\infty\int_0^{2\pi}\int_0^{2\pi} R_\lambda^*(r_i)R_\mu^*(r_j)\mathcal{H}_2R_\lambda(r_j)R_\mu(r_i)\mathrm{e}^{\mathrm{i}m(\phi_j-\phi_i)}\,\mathrm{d}\phi_j\,\mathrm{d}\phi_i\,r_j\,\mathrm{d}r_j\,r_i\,\mathrm{d}r_i,$$

where $m=m^\lambda-m^\mu$. Expanding the radial functions as in Eq. (19), we have to evaluate

$$\begin{aligned}\mathcal{I}_1 &= \frac{1}{4\pi^2}\sum_{i,j,p,q=0}^{\mathcal{N}-1} c_{i,m^\lambda}c_{j,m^\lambda}c_{p,m^\mu}c_{q,m^\mu} \\ &\quad\cdot\int_0^\infty\int_0^\infty\int_0^{2\pi}\int_0^{2\pi} v_{i,m^\lambda}(r_i)v_{p,m^\mu}(r_j)\mathcal{H}_2v_{j,m^\lambda}(r_i)v_{q,m^\mu}(r_j)\,\mathrm{d}\phi_j\,\mathrm{d}\phi_i\,r_j\,\mathrm{d}r_j\,r_i\,\mathrm{d}r_i,\end{aligned}$$

and

$$\begin{aligned}\mathcal{I}_2 &= \frac{1}{4\pi^2}\delta_{m_S^\lambda,m_S^\mu}\sum_{i,j,p,q=0}^{\mathcal{N}-1} c_{i,m^\lambda}c_{j,m^\lambda}c_{p,m^\mu}c_{q,m^\mu} \\ &\quad\cdot\int_0^\infty\int_0^\infty\int_0^{2\pi}\int_0^{2\pi} v_{i,m^\lambda}^*(r_i)v_{p,m^\mu}^*(r_j)\mathcal{H}_2v_{j,m^\lambda}(r_j)v_{q,m^\mu}(r_i)\mathrm{e}^{\mathrm{i}m(\phi_j-\phi_i)}\,\mathrm{d}\phi_j\,\mathrm{d}\phi_i\,r_j\,\mathrm{d}r_j\,r_i\,\mathrm{d}r_i.\end{aligned}$$

These integrals have already been computed, and are given by $\mathfrak{d}$, and $\mathfrak{f}$. So we get Eq. (28).

Appendix B. Analytic integrals

For convenience, when evaluating these below we will change variables, letting $x=kr^2$, and define the notation

$$\big\langle\{i,\alpha\},\{j,\beta\},m\big\rangle=\int_0^\infty \mathrm{e}^{-x}x^m L_i^\alpha(x)L_j^\beta(x)\,\mathrm{d}x.$$

The kinetic energy integrals given in Eq. (21) are evaluated as follows.

In[40] := **SetAttributes[*k*, Constant];**

$$In[41] := \mathbf{rule = c\_.L_{i\_}^{a\_}(x)L_{j\_}^{b\_}(x)x^{n\_\cdot} :\to \frac{e^x}{Dt[x]}\langle\{i,a\},\{j,b\},n\rangle c;}$$

$$In[42] := \Bigg(\Bigg(\Bigg(\frac{1}{2}v_{i,m}^{(0,1)}(k,r)v_{j,m}^{(0,1)}(k,r) + \frac{m^2}{2r^2}v_{i,m}(k,r)v_{j,m}(k,r)\Bigg)r \text{ // Expand}\Bigg)Dt[r]/.r \to \sqrt{\frac{x}{k}} \text{ //}$$
$$\text{Simplify // PowerExpand // Expand}\Bigg)/.\text{rule}$$

$$\begin{aligned}Out[42] = {} & \langle\{i-1,m+1\},\{j-1,m+1\},m+1\rangle k^{-m} - \tfrac{1}{2}m\langle\{i-1,m+1\},\{j,m\},m\rangle k^{-m}\\ & + \tfrac{1}{2}\langle\{i-1,m+1\},\{j,m\},m+1\rangle k^{-m} - \tfrac{1}{2}m\langle\{i,m\},\{j-1,m+1\},m\rangle k^{-m}\\ & + \tfrac{1}{2}\langle\{i,m\},\{j-1,m+1\},m+1\rangle k^{-m} + \tfrac{1}{2}m^2\langle\{i,m\},\{j,m\},m-1\rangle k^{-m}\\ & - \tfrac{1}{2}m\langle\{i,m\},\{j,m\},m\rangle k^{-m} + \tfrac{1}{4}\langle\{i,m\},\{j,m\},m+1\rangle k^{-m}\end{aligned}$$

The overlap integral given by Eq. (22) becomes

$$In[43] := \Bigg((v_{i,m}(k,r)v_{j,m}(k,r)r \text{ // Expand})Dt[r]/.r \to \sqrt{\frac{x}{k}} \text{ //}$$
$$\text{Simplify // PowerExpand // Expand}\Bigg)/.\text{rule}$$

$$Out[43] = \tfrac{1}{2}k^{-m-1}\langle\{i,m\},\{j,m\},m\rangle$$

The confining potential integrals given by Eq. (24), for the harmonic potential $V(r) = -V_0 + \frac{1}{2}k^2r^2$ become

$$In[44] := \mathbf{V_0 = .}$$

$$In[45] := \Bigg(\Big(\big(\tfrac{1}{2}k^2r^2 - V_0\big)v_{i,m}(k,r)v_{j,m}(k,r)r \text{ // Expand}\Big)Dt[r]/.r \to \sqrt{\frac{x}{k}} \text{ //}$$
$$\text{Simplify // PowerExpand // Expand}\Bigg)/.\text{rule}$$

$$Out[45] = \tfrac{1}{4}k^{-m}\langle\{i,m\},\{j,m\},m+1\rangle - \tfrac{1}{2}k^{-m-1}\langle\{i,m\},\{j,m\},m\rangle V_0$$

The evaluation of these integrals involving the generalized Laguerre polynomials is given below.

To compute the integral

$$\langle\{i,m\},\{j,m\},m\rangle = \int_0^\infty x^m e^{-x}L_i^m(x)L_j^m(x)\,dx,$$

we can immediately use the orthogonality relation for the generalized Laguerre polynomials [14], so that

$$\langle\{i,m\},\{j,m\},m\rangle = \delta_{i,j}\frac{\Gamma(m+i+1)}{i!} = \delta_{i,j}\frac{(m+i)!}{i!}.$$

It follows from this that

$$\langle\{i-1,m+1\},\{j-1,m+1\},m+1\rangle = \delta_{i-1,j-1}\frac{\Gamma((m+1)+(i-1)+1)}{(i-1)!} = \delta_{i,j}\frac{i(m+i)!}{i!}.$$

To compute the integral

$$\langle\{i,m\},\{j,m\},m+1\rangle = \int_0^\infty x^{m+1}e^{-x}L_i^m(x)L_j^m(x)\,dx,$$

we use the property $xL_i^\alpha(x) = -(i+\alpha)L_{i-1}^\alpha(x) - (i+1)L_{i+1}^\alpha(x) + (2i+\alpha+1)L_i^\alpha(x)$ [14], so that

$$\begin{aligned}
\big\langle\{i,m\},\{j,m\},m+1\big\rangle &= \int_0^\infty x^{m+1}\mathrm{e}^{-x}L_i^m(x)L_j^m(x)\,\mathrm{d}x \\
&= -(i+m)\big\langle\{i-1,m\},\{j,m\},m\big\rangle + (2i+m+1)\big\langle\{i,m\},\{j,m\},m\big\rangle \\
&\quad -(i+1)\big\langle\{i+1,m\},\{j,m\},m\big\rangle \\
&= -(i+m)\delta_{i-1,j}\tfrac{\Gamma(m+i)}{j!} + (2i+m+1)\delta_{i,j}\tfrac{\Gamma(m+i+1)}{i!} - (i+1)\delta_{i+1,j}\tfrac{\Gamma(m+i+2)}{(i+1)!} \\
&= -\delta_{i-1,j}\tfrac{\Gamma(m+j+2)}{j!} + \delta_{i,j}(2j+m+1)\tfrac{\Gamma(m+j+1)}{j!} - \delta_{i,j-1}\tfrac{j\Gamma(m+j+1)}{j!} \\
&= \tfrac{(m+j)!}{j!}\big((2j+m+1)\delta_{i,j} - (m+j+1)\delta_{i-1,j} - j\delta_{i,j-1}\big).
\end{aligned}$$

To compute the integral

$$\big\langle\{i,m\},\{j,m\},m-1\big\rangle = \int_0^\infty x^{m-1}\mathrm{e}^{-x}L_i^m(x)L_j^m(x)\,\mathrm{d}x,$$

we use the property $L_i^{\alpha+1}(x) = \sum_{k=0}^i L_k^\alpha(x)$ [14], so that

$$\begin{aligned}
\big\langle\{i,m\},\{j,m\},m-1\big\rangle &= \int_0^\infty x^{m-1}\mathrm{e}^{-x}L_i^m(x)L_j^m(x)\,\mathrm{d}x, \\
&= \sum_{n=0}^i\sum_{k=0}^j\big\langle\{n,m-1\},\{k,m-1\},m-1\big\rangle \\
&= \sum_{n=0}^i\sum_{k=0}^j\delta_{n,k}\frac{\Gamma(m+n)}{n!} = \sum_{n=0}^{\mathrm{Min}(i,j)}\frac{\Gamma(m+n)}{n!} \\
&= \frac{\Gamma(m+\mathrm{Min}(i,j)+1)}{m\Gamma(\mathrm{Min}(i,j)+1)} = \begin{cases}\frac{(m+i)!}{m\,i!} & j\geqslant i,\\ \frac{(m+j)!}{m\,j!} & j<i.\end{cases}
\end{aligned}$$

(Note that this term is multiplied by m^2, so there is no problem when $m=0$.)

To compute the integral

$$\big\langle\{i,m\},\{j-1,m+1\},m\big\rangle = \int_0^\infty x^m\mathrm{e}^{-x}L_i^m(x)L_{j-1}^{m+1}(x)\,\mathrm{d}x,$$

we use the property $L_i^{\alpha+1}(x) = \sum_{k=0}^i L_k^\alpha(x)$ [14], so that

$$\begin{aligned}
\big\langle\{i,m\},\{j-1,m+1\},m\big\rangle &= \int_0^\infty x^m\mathrm{e}^{-x}L_i^m(x)L_{j-1}^{m+1}(x)\,\mathrm{d}x \\
&= \sum_{k=0}^{j-1}\big\langle\{i,m\},\{k,m\},m\big\rangle = \sum_{k=0}^{j-1}\delta_{i,k}\frac{\Gamma(m+i+1)}{i!} \\
&= \begin{cases}\frac{\Gamma(m+i+1)}{i!}, & 0\leqslant i\leqslant j-1\\ 0, & i\geqslant j\end{cases} = \theta(j-i-1)\frac{(m+i)!}{i!},
\end{aligned}$$

where

$$\theta(x) = \begin{cases} 1, & x \geqslant 0 \\ 0, & x < 0 \end{cases}$$

is the Heaviside step function. By symmetry, we can also say that

$$\big\langle \{i-1, m+1\}, \{j, m\}, m \big\rangle = \theta(i-j-1)\frac{(m+j)!}{j!}.$$

To compute the integral

$$\big\langle \{i, m\}, \{j-1, m+1\}, m+1 \big\rangle = \int_0^\infty x^{m+1} \mathrm{e}^{-x} L_i^m(x) L_{j-1}^{m+1}(x)\,\mathrm{d}x,$$

we use the property $L_i^{\alpha-1}(x) = L_i^\alpha(x) - L_{i-1}^\alpha(x)$ [14], so that

$$\begin{aligned}
&\big\langle \{i, m\}, \{j-1, m+1\}, m+1 \big\rangle \\
&\quad = \int_0^\infty x^{m+1} \mathrm{e}^{-x} L_i^m(x) L_{j-1}^{m+1}(x)\,\mathrm{d}x \\
&\quad = \big\langle \{i, m+1\}, \{j-1, m+1\}, m+1 \big\rangle - \big\langle \{i-1, m+1\}, \{j-1, m+1\}, m+1 \big\rangle \\
&\quad = \delta_{i,j-1}\frac{\Gamma(m+i+2)}{i!} - \delta_{i-1,j-1}\frac{\Gamma(m+i+1)}{(i-1)!} \\
&\quad = \delta_{i,j-1}\frac{\Gamma(m+i+2)}{i!} - \delta_{i,j}\frac{i\Gamma(m+i+1)}{i!} \\
&\quad = \frac{(m+i)!}{i!}\big((m+i+1)\delta_{i,j-1} - i\delta_{i,j}\big).
\end{aligned}$$

By symmetry, we can also say that

$$\begin{aligned}
\big\langle \{i-1, m+1\}, \{j, m\}, m+1 \big\rangle &= \delta_{i-1,j}\frac{\Gamma(j+m+2)}{j!} - \delta_{i,j}\frac{j\Gamma(j+m+1)}{j!} \\
&= \frac{(m+j)}{j!}\big((m+j+1)\delta_{i-1,j} - j\delta_{i,j}\big).
\end{aligned}$$

Combining these results we obtain a tridiagonal matrix for the kinetic energy integrals, and a diagonal matrix for the overlap integrals (§3.3).

Appendix C. Gaussian integral

When considering a Gaussian function of the form $V(r) = -V_0 \mathrm{e}^{-r^2/R^2}$, the confining potential integral given by Eq. (24) becomes

$$-V_0 \int_0^\infty \mathrm{e}^{-r^2/R^2} v_{i,m}^*(r) v_{j,m}(r) r\,\mathrm{d}r.$$

Changing variables, so that $x = kr^2$ (where $k = \sqrt{2V_0/R^2}$), this integral becomes an integral over $r = [0, \infty)$ with integrand determined as follows.

In[46] := **SetAttributes[{*R*, *β*}, Constant];**

In[47] := $-\mathbf{V_0 e^{-r^2/R^2} v_{i,m}(k,r) v_{j,m}(k,r) r\,Dt[r]\ /.\ r \to \sqrt{\frac{x}{k}}\ //\ Simplify\ //\ PowerExpand}$

Out[47] = $-\frac{1}{2}\mathrm{e}^{(-1-\frac{1}{R^2 k})x} k^{-m-1} x^m \,\mathrm{d}x\, L_i^m(x) L_j^m(x) V_0$

Dividing through by $-\frac{V_0}{2}k^{-m-1}$, defining $\beta = kR^2$, and changing variables again so that $x \to \beta x$, this becomes

In[48] := $\mathbf{\frac{\%}{-\frac{V_0}{2}k^{-m-1}}\ /.\ First\big[Solve[\beta == kR^2, k]\big]\ /.\ x \to \beta x\ //\ PowerExpand\ //\ Simplify}$

Out[48] = $\mathrm{e}^{-x(\beta+1)} x^m \beta^{m+1} \,\mathrm{d}x\, L_i^m(x\beta) L_j^m(x\beta)$

Dividing through by β^{m+1}, defining $\gamma = \beta/(\beta+1)$, and changing variables once more so that $x \to \gamma x$, we get

In[49] := $\mathbf{\left(\frac{\%}{\beta^{m+1}}\ /.\ x \to \frac{x}{\beta+1}\ /.\ First\left[Solve\left[\gamma == \frac{\beta}{\beta+1}, \beta\right]\right]\ //\ Simplify\right)\ /.}$
$\mathbf{\{(\gamma-1) \to -(1-\gamma), (x - x\gamma) \to x(1-\gamma)\}\ //\ PowerExpand\ //\ Simplify}$

Out[49] = $\mathrm{e}^{-x} x^m (1-\gamma)^{m+1} \,\mathrm{d}x\, L_i^m(x\gamma) L_j^m(x\gamma)$

So we want to evaluate

$$-\frac{V_0}{2}\left(\frac{\beta(1-\gamma)}{k}\right)^{m+1} \int_0^\infty x^m \mathrm{e}^{-x} L_i^m(\gamma x) L_j^m(\gamma x)\,\mathrm{d}x.$$

Now, the Laguerre polynomials can be written as [20, Eq. (1) of §1.7]

$$L_n^\alpha(x) = \binom{n+\alpha}{n} {}_1F_1(-n; \alpha+1; x),$$

where ${}_1F_1(-n;\alpha+1;x)$ is the Kummer confluent hypergeometric function. We can then use the integral identity [20, Eq. (29) of §9.4]

$$\int_0^\infty \mathrm{e}^{-t} t^{\alpha-1} {}_1F_1(\beta;\gamma;xt)\, {}_1F_1(\beta';\gamma';yt)\,\mathrm{d}t = \Gamma(\alpha) F_2[\alpha;\beta,\beta';\gamma,\gamma';x,y],$$

where $F_2[\alpha;\beta,\beta';\gamma,\gamma';x,y]$ is the Appell hypergeometric function of the second kind. So

$$\begin{aligned}\int_0^\infty x^m \mathrm{e}^{-x} L_i^m(\gamma x) L_j^m(\gamma x)\,\mathrm{d}x &= \binom{i+m}{i}\binom{j+m}{j}\int_0^\infty \mathrm{e}^{-x} x^m\, {}_1F_1(-i;m+1;\gamma x)\, {}_1F_1(-j;m+1;\gamma x)\,\mathrm{d}x \\ &= \frac{(i+m)!(j+m)!}{i!j!m!} F_2[m+1;-i,-j;m+1,m+1;\gamma,\gamma].\end{aligned}$$

Further simplification is possible using the identity [20, Eq. (108) of §9.4]

$$F_2[\alpha;\beta,\beta';\alpha,\alpha;x,y] = (1-x)^{-\beta}(1-y)^{-\beta'}\, {}_2F_1\left(\beta,\beta';\alpha;\frac{xy}{(1-x)(1-y)}\right),$$

where ${}_2F_1(\beta,\beta';\alpha;\frac{xy}{(1-x)(1-y)})$ is the Gauss hypergeometric function. Therefore

$$\int_0^\infty x^m \mathrm{e}^{-x} L_i^m(\gamma x) L_j^m(\gamma x)\,\mathrm{d}x = \frac{(i+m)!(j+m)!}{i!j!m!}(1-\gamma)^{i+j}\, {}_2F_1\left(-i,-j;m+1;\frac{\gamma^2}{(\gamma-1)^2}\right).$$

So finally, the integral we want is

$$-\frac{V_0}{2}\left(\frac{\beta}{k}\right)^{m+1}\frac{(i+m)!(j+m)!}{i!j!m!}(1-\gamma)^{i+j+m+1}\,{}_2F_1\left(-i,-j;m+1;\frac{\gamma^2}{(\gamma-1)^2}\right).$$

In terms of k and V_0 this is

$$\begin{aligned}In[50]:=&\left(-\frac{V_0}{2}\left(\frac{\beta}{k}\right)\frac{(i+m)!(j+m)!}{i!j!m!}(1-\gamma)^{i+j+m+1}\,{}_2F_1\left(-i,-j;m+1;\frac{\gamma^2}{(\gamma-1)^2}\right)\text{ /.}\right.\\&\gamma\to\frac{\beta}{\beta+1}\text{ /. }\beta\to kR^2\text{ /. }R\to\sqrt{\frac{2V_0}{k^2}}\text{ // Simplify}\Bigg)\text{ /.}\\&(k+2V_0)\to k\left(\frac{2V_0}{k}+1\right)\text{ // PowerExpand // Simplify}\end{aligned}$$

$$Out[50]=-\frac{2^m k^{-2(m+1)}(i+m)!(j+m)!\,{}_2F_1\left(-i,-j;m+1;\frac{4V_0^2}{k^2}\right)V_0^{m+2}\left(\frac{2V_0}{k}+1\right)^{-i-j-m-1}}{i!j!m!}$$

The Gaussian confining potential integral is then implemented as

```
In[51]:= Clear[V];
In[52]:= V /: V_(i_,j_)
      := V /: V_(i,j) = V /: V_(j,i)
       = Function[{k, V0, m},
           -(2^m V0^(m+2))/k^(2(m+1)) ((i+m)!(j+m)!)/(i!j!m!) (1+(2V0)/k)^(-i-j-m-1)
             2F1[-i, -j; m+1; (4V0^2)/k^2]]
```

References

[1] L. Kouwenhoven, C. Marcus, Phys. World (1998) 35.
[2] R.C. Ashoori, Nature 379 (1996) 413.
[3] M.A. Reed, Scientific Amer. (1993) 98.
[4] D. Gammon, Nature 405 (2000) 899.
[5] D.P. DiVincenzo, G. Burkard, D. Loss, in: I.O. Kulik (Ed.), Quantum Mesoscopic Phenomena and Mesoscopic Devices in Microelectronics, NATO Advanced Study Institute, Turkey, 1999.
[6] V. Fock, Z. Phys. 47 (1928) 446.
[7] C.G. Darwin, Proc. Cambridge Philos. Soc. 27 (1930) 86.
[8] D. Pfannkuche, V. Gudmundsson, P. Maksym, Phys. Rev. B 47 (1993) 2244.
[9] T. Ezaki, Y. Sugimoto, N. Mori, C. Hamaguchi, Semicond. Sci. Technol. 13 (1998) A1.
[10] I. Lee, V. Rao, R. Martin, J. Leburton, Phys. Rev. B 57 (1998) 9035.
[11] S. Tarucha, D.G. Austing, T. Honda, R.J. van der Hage, L.P. Kouwenhoven, Phys. Rev. Lett. 77 (1996) 3613.
[12] T. Ezaki, N. Mori, C. Hamaguchi, Phys. Rev. B 56 (1997) 6428.
[13] S. Sahrakorpi, Interface and manual for demonstrating the Schrödinger wave equation in two dimensions with Matlab, Tampere University of Technology, 1996, http://alpha.cc.tut.fi/∼sahrakor/research/teksti/teksti.html.
[14] M. Abramowitz, I.A. Stegun, Handbook of Mathematical Functions: With Formulas, Graphs and Mathematical Tables, Dover, New York, 1965.
[15] B.H. Bransden, C.J. Joachain, Physics of Atoms and Molecules, Longman, New York, 1983.
[16] J. Adamowski, M. Sobkowicz, B. Szafran, S. Bednarek, Phys. Rev. B 62 (2000) 4234.
[17] E.W. Weisstein, Eric Weisstein's World of Mathematics, Wolfram Research, 1996–2000, http://mathworld.wolfram.com/.
[18] C. Fischer, T. Brage, P. Jönsson, Computational Atomic Structure: An MCHF Approach, IOP, Bristol, 1997.
[19] R.D. Cowan, The Theory of Atomic Structure and Spectra, University of California Press, Berkeley, 1981.
[20] H.M. Srivastava, P.W. Karlsson, Multiple Gaussian Hypergeometric Series, Ellis Horwood Ltd., Chichester, 1985.